PLATE BUCKLING ANALYSIS USING LINEAR AND NON-LINEAR FINITE ELEMENT METHODS

by

Thomas Persson

Submitted in Partial Fulfillment of the Requirements

for the Degree of

Master of Science in Engineering

in the

Mechanical Engineering

Program

YOUNGSTOWN STATE UNIVERSITY

August, 1996

PLATE BUCKLING ANALYSIS USING LINEAR AND

NON-LINEAR FINITE ELEMENT METHODS

Thomas Persson

I hereby release this thesis to the public. I understand this thesis will be housed at the Circulation Desk of the University library and will be available for public access. I also authorize the University or other individuals to make copies of this thesis as needed for scholarly research.

Signature:

Thomas P — 7/16/96

Student — Date

Approvals:

Thesis Advisor — 7/16/96 — Date

Committee Member — 7/16/96 — Date

Committee Member — 7/16/96 — Date

Dean of Graduate Studies — 8/1/96 — Date

ABSTRACT

The objective of this study was to develop new design charts for linear elastic buckling coefficients of rectangular flat plates with support conditions not previously found in the literature. Critical buckling coefficients were found for rectangular flat plates subjected to uniform compression with partially supported unloaded edges using the finite element method. Plates with different aspect ratios and with varying support length on the unloaded edge were analyzed. Currently there are no design charts available in the literature for plates subjected to uniform compression and with partially supported unloaded edges. An engineer will be able to use these new design charts in the design work of structures that are susceptible to instability failures. The method developed in this work was verified on problems where closed form mathematical solutions exist.

A second part of this study was to investigate the effect of initial plate imperfections on the ultimate plate strength with the use of a non-linear finite element method. By using a non-linear finite element method, it is possible to model both an initial imperfection and post yield elasto-plastic conditions. Plates that are failing by a combination of buckling and yielding with initial geometric imperfections are analyzed. The results obtained from the non-linear finite element method were compared to an approximate method available in the literature.

ACKNOWLEDGMENTS

The author would like to take this opportunity to thank the following people for their support:

Dr. Daniel H. Suchora - Advisor

Dr. Frank J. Tarantine - Graduate Committee

Dr. Jeffrey L. Ray - Graduate Committee

Marc Pentecost - Graduate student, Youngstown State University

Anthony Viviano - Graduate student, Youngstown State University

Wendy Persson - my wife without whom this work would not have been possible

TABLE OF CONTENTS

LIST OF FIGURES

NOMENCLATURE

a	length of the plate (in)
a'	supported length of an unloaded, longitudinal edge
b	width of plate (in)
b_e	"effective-width"
D	$\frac{Et^3}{12(1-\nu^2)}$; flexural rigidity of the plate (lb*in)
{d}	global nodal displacement vector
E	Young's modulus (psi)
E_T	tangent modulus (strain-hardening modulus) (psi)
ΔF	unbalanced nodal force vector
{F}	global nodal force vector
g	gap between intermittent supports (in)
I_s	moment of inertia of a stiffener (in^4)
[K]	global stiffness matrix
K	buckling coefficient (--)
K'	$K\pi^2/12$ (--)
K_s	buckling coefficient for shear buckling stress (--)
K_L	linear stiffness matrix
K_G	geometric stiffness matrix
M_y	edge moment along the x-axis (in*lb)
M_{xy}	twisting moment (in*lb)
N_x	edge force per unit length in the x-direction (lb/in)
N_y	edge force per unit length in the y-direction (lb/in)
N_{xy}	edge shearing force per unit length (lb/in)
P_{ult}	ultimate load (lb)

Q_x	shearing force (lb)
$q(x,y)$	intensity of a distributed lateral load (lb)
ΔT_1	work done by external forces (lb*in)
t	thickness of plate (in)
ΔU	strain energy of bending (lb*in)
U_n	global displacement vector (non-linear finite element method)
V_e	total potential energy of a plate element (lb*in)
w	displacement function (in)
z	distance from neutral surface (in)
α	the ratio a/b (--)
δ	nodal displacement vector
ε_D	displacement tolerance (--)
ε_x	strain in the x-direction (--)
ε_y	strain in the y-direction (--)
ϕ	a/b
γ_{xy}	shear strain (--)
γ	$\frac{EI_s}{bD}$ (--)
λ_{cr}	buckling load factor
ν	Poisson's ratio (--)
$1/\rho_x$	curvature of the neutral surface in a section parallel to the xz-plane (in)
$1/\rho_y$	curvature of the neutral surface in a section parallel to the yz-plane (in)
σ_C	critical buckling stress (psi)
σ^*_C	critical stress for the case with compression only (psi)
σ_{Cb}	compressive stress due to bending (psi)
σ^*_{Cb}	critical buckling stress for bending (psi)
σ_x	normal stress in the x-direction (psi)
σ_y	normal stress in the y-direction (psi)

σ_y	yield point of the material under consideration (psi)
σ_{VM}	von Mises equivalent 1-D stress (psi)
$\sigma_{1,2,3}$	principal stresses (psi)
σ_e	edge stress (psi)
σ_{av}	average stress at ultimate load
τ_c	critical shear stress (psi)
τ^*_c	critical stress for the case with shear only (psi)
τ_{xy}	shear stress (psi)

1. INTRODUCTION

Linear elastic buckling of plates that are subjected to in-plane forces is a problem of great practical importance that has been extensively researched over the past 60 years. Elastic instability of flat rectangular plates became an important research area when the design of the lightweight airframes was introduced. Later, the theory of thin plates has been applied to engineering structures (Fok, 1984). Some advantages of thin-walled structures' are high strength coupled with the ease of manufacturing and the relative low weight. However, thin-walled structures have the characteristic of susceptibility of failure by instability or buckling. It is therefore important to the design engineer that accurate methods are available to determine the critical buckling strength.

Most research on instability of flat plates has been done on rectangular shapes of various proportions. Usually the plates are supported continuously along all edges with loading occurring along two opposite sides. A limited amount of work has been done on plates with an unsupported or partially supported unloaded edges.

Norris, et. al., (1951) studied the buckling behavior of intermittently supported rectangular plates with both analytical methods and laboratory experiments. The buckling of simply supported but partially clamped rectangular plates subjected to uniform compression was studied by Hamada et. al., (1967). Hamada et. al. used the energy method and laboratory experiments to investigate this problem.

According to Wang et. al. (1993) engineers tend to use design charts and formulas rather than using accurate but more complex solution methods such as finite element analysis in everyday design work. Approximate formulas and design charts will continue to be used until inexpensive and much more user-friendly computer software are available to all engineers.

The objective of this study was to develop new design charts for the linear elastic critical buckling stress of rectangular isotropic flat plates with one partially supported unloaded edge using the finite element method. A second part of this study was to

investigate the effect the initial imperfection has on the ultimate strength of the plate, by the use of a non-linear finite element method.

As mentioned earlier, only a few published papers investigate the problem of flat plates subjected to uniform compression with non-continuous boundary conditions. An example of a problem could be a welded plate structure with openings. As an example, consider the web of an I-section under compression where the top flange is shorter than the bottom flange.

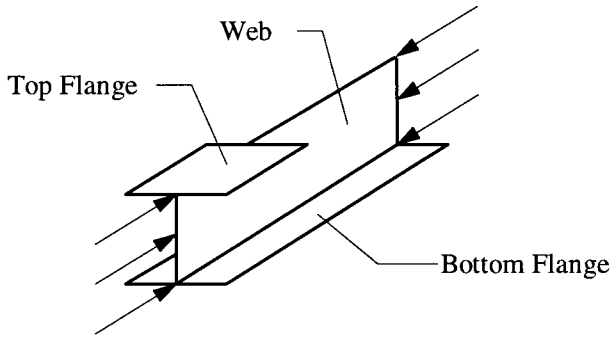

Figure 1: I-beam under compression.

In this case the web is only supported partially by the top flange, but fully supported by the bottom flange. Currently there are no design charts or formulas that include buckling coefficients for the above case. This paper presents buckling coefficients for cases with partially supported unloaded edges.

In this work, buckling coefficients and the ultimate strength of flat plates are obtained by using the finite element method. The linear elastic buckling stress was obtained using a linear eigenvalue buckling analysis solver. Verification of the finite element method was done by comparing to closed-form solutions.

The second part of the finite element analysis consisted of an investigation on the effect initial imperfections had on the ultimate strength of the plate. The ultimate strength of the plate was obtained by using a non-linear finite element analysis procedure. The non-linear finite element method has the advantage over a linear finite element method in that it can model initial imperfections and post-yield elasto-plastic conditions. The

ultimate strength of the flat plate was found when a small increase in the load resulted in a very large deflection of the plate, i.e., the stiffness of the plate approached zero. This method was verified using a flat plate whose ultimate strength was known from an approximate method, the "effective-width" method.

A literature review of previous research of buckling of flat plates is presented in the next section. Then in chapter 3 and 4, the theories of thin plates and elastic stability are reviewed. Chapter 5 presents the finite element analysis and the results that were obtained. A conclusion and a discussion of the results are included in chapter 6.

2. LITERATURE REVIEW

Numerous research studies have been done over the years for rectangular plates with different boundary and loading conditions (Timoshenko, 1936 and Bulson, 1970). Bryan (1891) presented what seems to be the first published paper on elastic critical stress. Bryan analyzed a rectangular flat plate under uniform compression with simply supported edges. Over the years different combinations of simply supported and clamped edges have been studied. Different loading conditions have been, for example, uniform compression, bending and shear. The elastic critical stress is a function of the material (E, ν), the width (b), thickness (t) and the boundary conditions. The elastic critical stress is given by (Timoshenko, 1936):

$$\sigma_c = K \times \frac{\pi^2 E}{12\left(1-\nu^2\right)\left(\frac{b}{t}\right)^2} \qquad \textbf{Eq. 1}$$

where: σ_c = critical buckling stress

K = buckling coefficient

E = Young's modulus

ν = Poisson's ratio

b = width of the plate (See Figure 2 below)

t = thickness of the plate (See Figure 2 below)

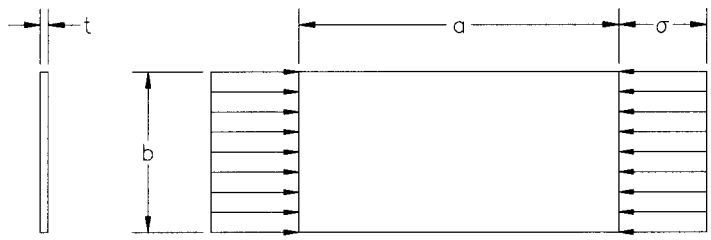

Figure 2: Sketch of a flat plate under compression.

Note: In this work, the factor $\pi^2/12$ is embedded in the buckling coefficient i. e., the buckling coefficient is defined as: $K' = K\pi^2/12$.

2.1 Flat plates under uniform compression

Shown below are flat plates under uniform compression with different types of boundary conditions:

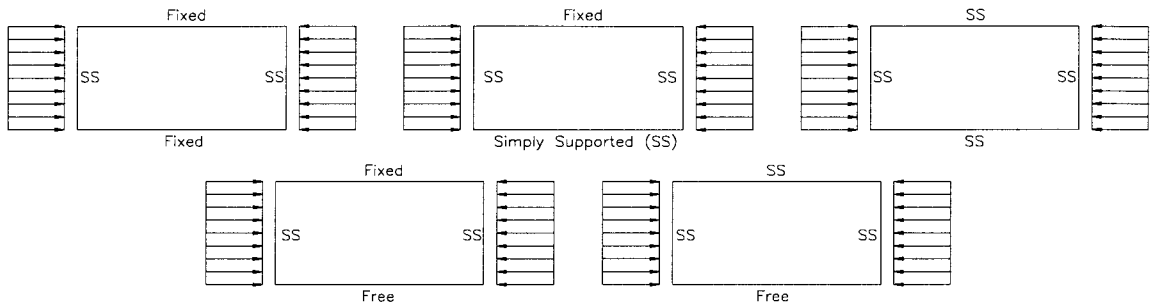

Figure 3: Flat plates under uniform compression.

Timoshenko (1936) studied all of the above cases and Heck and Ebner (1936) and Maulbetsch (1937) investigated cases when edges were fixed.

2.2 Flat plates under combined bending and compressive stresses

Buckling stresses for flat plates in compression and bending have been investigated by Timoshenko (1936), Heck and Ebner (1936), Bijlaard (1957) and Brockenbrough and Johnston (1974). In this case the plate is subjected to a combination of compression and bending and the compressive stress along the edges will vary from a maximum to a minimum, as shown below:

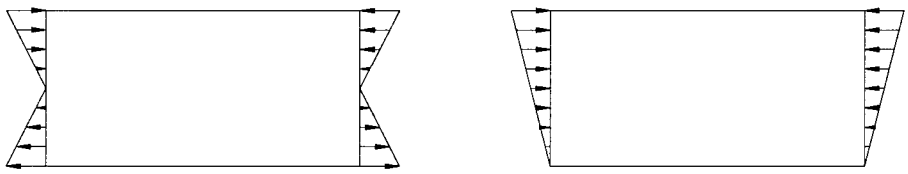

Figure 4: Combined bending and compression of a flat plate.

Minimum buckling coefficients were published by Galambos (1988) for the following ratios between bending stress and compressive stress, for plates with simply supported edges:

$$\frac{\sigma_{cb}}{\sigma_c} = \infty, 5.00, 2.00, 1.00, 0.50, 0.0$$

where: σ_{cb} = compressive stress due to bending

σ_c = compressive stress due to uniform compression

The first case corresponds to pure bending and the last case to pure compression. For plates with fixed unloaded edges and for plates with one free edge, minimum buckling coefficients were given for $\sigma_{cb}/\sigma_b = \infty$, 1.00 and 0.0.

2.3 Flat plates under uniform compression / tension in two perpendicular directions

For the case of a flat plate under uniform compression or tension in two perpendicular directions with simply supported edges (as shown below), research has been done by Timoshenko (1936) and Heck and Ebner (1936). Timoshenko (1936) also studied the cases with clamped edges.

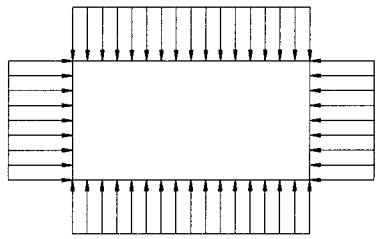

Figure 5: Rectangular plate under uniform compression in two perpendicular directions.

2.4 Combined bending and compressive stresses in two perpendicular directions

The case of combined bending and compressive stresses in two perpendicular directions for a rectangular plate, buckling coefficients have been published by Yoshizuka and Narmoka (1971).

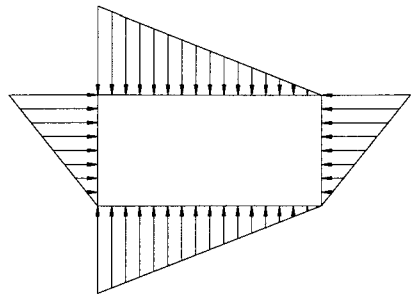

Figure 6: Flat plate subjected to compression and bending in two perpendicular directions.

2.5 Rectangular plates subjected to edge shear stresses on all edges

The plate shown below is subjected to edge shear stresses on all edges, this stress state is called "pure shear".

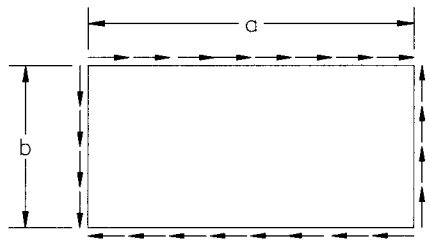

Figure 7: Plate subjected to pure shear .

For the case with a plate with all edges simply supported, critical buckling coefficients were developed by Timoshenko (1910), Bergmann and Reissner (1932) and Seydel (1933). The critical shear stress can be found by substituting τ_c and K_s for σ_c and K in Eq. 1. Approximate expressions for the critical buckling coefficient, K_s are given below:

$$K_s = 4.00 + \frac{5.34}{\alpha^2} \qquad \text{valid for } \alpha \leq 1$$

$$K_s = 5.34 + \frac{4.00}{\alpha^2} \qquad \text{valid for } \alpha \geq 1$$

where: $\alpha = a/b$

For a plate with all edges clamped, Moheit (1939) developed the following expressions for the critical buckling coefficient:

$$K_s = 5.6 + \frac{8.98}{\alpha^2} \qquad \text{valid for } \alpha \leq 1$$

$$K_s = 8.98 + \frac{5.6}{\alpha^2} \qquad \text{valid for } \alpha \geq 1$$

The case for a plate with two opposite edges clamped and the other two edges simply supported, Iguchi (1938) developed a solution for a general rectangular plate and Leggett (1941) for a square plate.

2.6 Shear combined with direct stress

Iguchi (1938) investigated the case with a plate subjected to shear and uniform compression with all edges simply supported. Shown below is a plate subjected to shear and uniform compression.

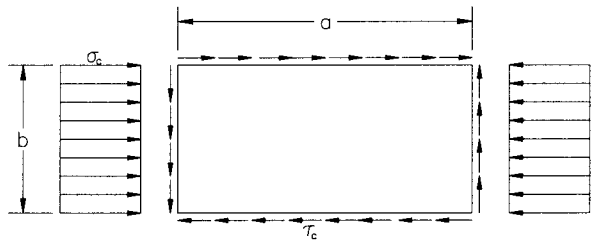

Figure 8: Plate subjected to shear and uniform compression.

Iguchi developed an approximate interaction equation between the critical buckling stress for uniform compression and for shear alone. This interaction equation given below predicts instability when satisfied.

$$\frac{\sigma_c}{\sigma_c^*} + \left(\frac{\tau_c}{\tau_c^*}\right)^2 = 1 \qquad \text{valid for } \frac{a}{b} > 1$$

where: σ^*_c = critical stress for the case with compression only

τ^*_c = critical stress for the case with shear only

σ_c = actual compression stress present

τ_c = actual shearing stress present

2.7 Shear combined with bending

A plate that is subjected to a combination of pure shear and pure bending is shown below:

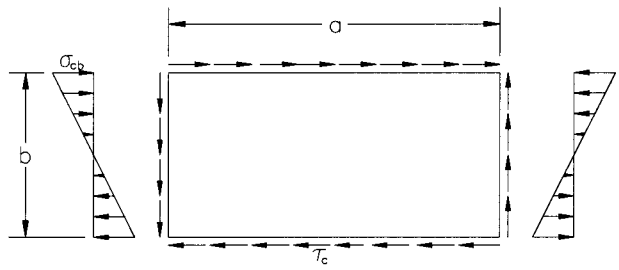

Figure 9: Plate subjected to shear and bending.

Timoshenko (1934) investigated this problem and presented a reduced critical buckling coefficient, k_c which is a function of τ_c / τ^*_c. This value for k_c is valid for $\alpha = 0.5$, 0.8 and 1.0.

where: $\alpha = a/b$

τ_c = the actual shearing stress present

τ^*_c = the buckling stress for pure shear

Stein (1936) and Way (1936) also investigated this case. Chwalla (1936) presented the following approximate interaction formula predicting failure, which corresponds well with the results from Stein and Way.

$$\left(\frac{\sigma_{cb}}{\sigma^*_{cb}}\right)^2 + \left(\frac{\tau_c}{\tau^*_c}\right)^2 = 1$$

where: σ^*_{cb} = the critical buckling stress for bending

σ_{cb} = the actual bending stress present

τ_c = the actual shearing stress present

τ^*_c = the critical buckling stress for pure shear

2.8 Shear combined with bending and uniform compression

For a plate which is subjected to a combination of shear, bending and compression and having all four edges simply supported (as shown below), an interaction formula was presented by Gerard and Becker (1957/1958).

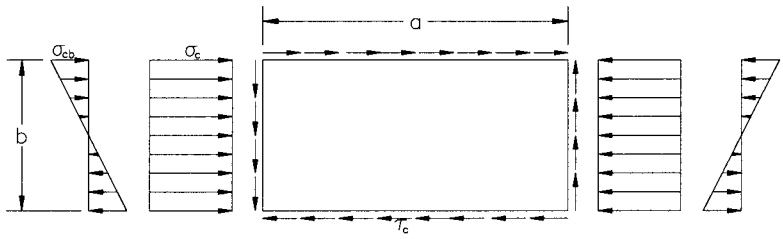

Figure 10: Plate subjected to shear, compression and bending.

The three-part interaction formula is given by:

$$\left(\frac{\sigma_c}{\sigma^*_c}\right) + \left(\frac{\sigma_{cb}}{\sigma^*_{cb}}\right)^2 + \left(\frac{\tau_c}{\tau^*_c}\right)^2 = 1$$

where: σ^*_c = the critical buckling stress for compression

σ_c = the actual compression stress present

McKenzie (1964) presented interaction graphs that took into account, in addition to the above loading condition, a uniform compressive load applied on the horizontal edge, as shown below.

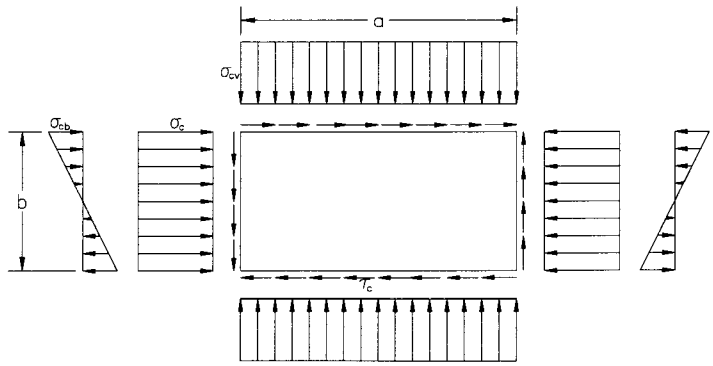

Figure 11: Plate subjected to compression, bending, shear and a vertical applied compression loading.

2.9 Buckling strength of stiffened plates: Uniaxial compression, combined compression and shear

To increase the stiffness of a plate, stiffeners can be added, as shown below. Both longitudinal and transverse stiffeners are used, either separately or in a combination.

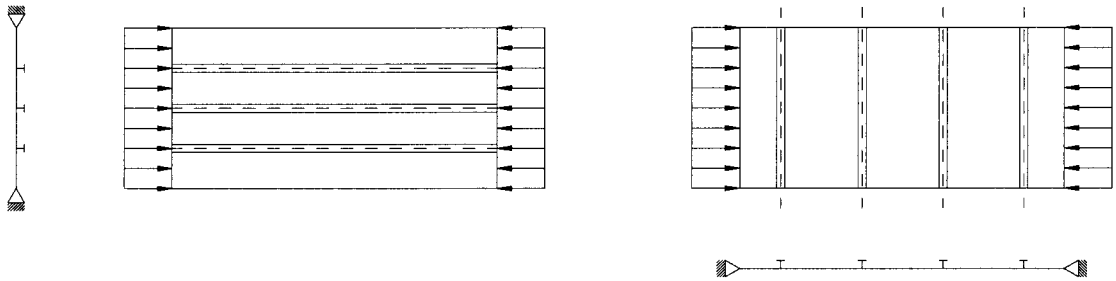

Figure 12: Plates with longitudinal and transverse stiffeners.

For the case with longitudinal stiffeners, Timoshenko and Gere (1961), Bleich and Ramsey (1951) and Seide and Stein (1949) have presented solutions to plates with one, two or three longitudinal stiffeners equally spaced (parallel to the applied loading). Graphs and tables are given by the authors above to determine the critical stress for plates simply supported on all edges.

Timoshenko and Gere (1961) investigated plates in uniaxial compression with transverse stiffeners. For one, two or three equally spaced transverse stiffeners, Timoshenko and Gere defined the required size of the stiffeners. Klitchieff (1949) defined

the required size of stiffeners when any number of stiffeners are used. Gerard and Becker (1957/1958) investigated the case with both longitudinal and transverse stiffeners and supplied the minimum value of γ as a function of α for different combinations of longitudinal and transverse stiffeners in graphs.

where: $\gamma = \frac{EI_s}{bD}$

EI_s = flexural rigidity of one transverse stiffener

$D = \frac{Et^3}{12(1-\nu^2)}$; flexural rigidity of the plate

$\alpha = \frac{a}{b}$

2.10 Buckling strength of flat plates with partial boundary conditions

To this author's knowledge there are just a few papers published on the buckling of rectangular plates with partially edge boundary conditions (Hamada et. al. 1967 and Norris et. al. 1951).

2.10.1 Flat plate under uniform compression with simply supported but partially clamped edges.

Hamada et. al. (1967) investigated flat plates in uniform compression with simply supported loaded edges and simply supported but partially clamped unloaded edges.

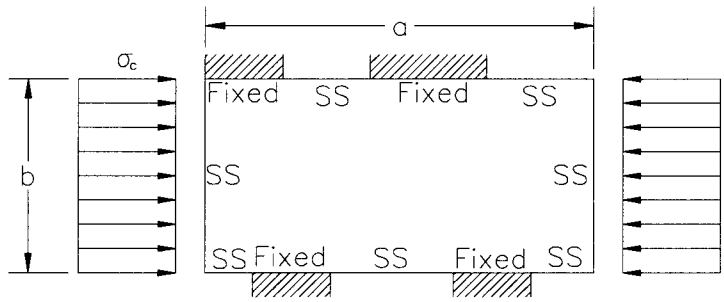

Figure 13: Flat plate under uniform compression with simply supported but partially clamped unloaded edges and simply supported loaded edges.

An energy method proposed by Hamada and Ota (1958, 1959) was used to investigate this problem. Ten cases were presented with diagrams for plates with aspect ratio 1, 2/3 and 1/2. Verification of the results were done by laboratory experiments.

2.10.2 Flat plate under compression with intermittently simply supported edges.

Norris et. al. (1951) studied the buckling behavior of long rectangular plates intermittently supported along the unloaded edges. Shown below is a sketch of the intermittently supported plate.

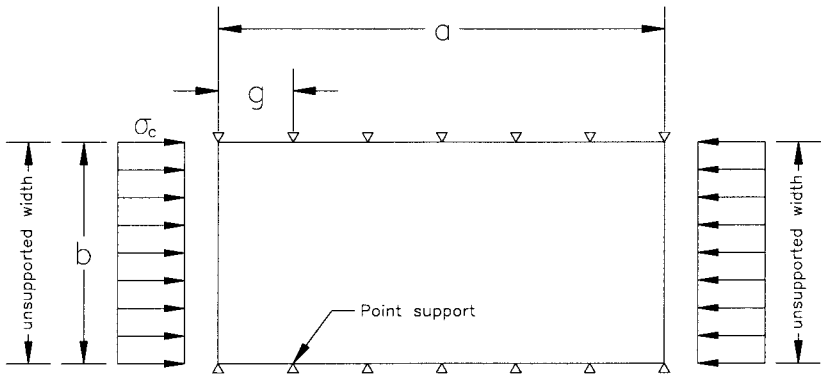

Figure 14: Long flat plate with intermittently simply supported edges.

The objective of their research was to develop specifications that could be used to determine the required length of intermittent fillet welds to connect component parts of structural members. The critical buckling coefficient, K was given as follows of Norris et. al.:

$K = 4.0$ valid for $0 < g/b < 0.5$

$K = (b/g)^2$ valid for $g/b > 0.5$

where: b = unsupported width of the plate

g = gap between intermittent supports

Norris et. al. also presented experimental results together with theoretical data.

3. PLATE THEORY

A summary of the elastic bending and buckling theory of thin plates is discussed next. This summary gives the needed theoretical background to elastic bending and buckling of flat plates and to the mathematical definitions of the boundary conditions. These definitions will be referred back to in Chapter 5 in the finite element modeling of the plates in this paper.

3.1 Basic assumptions used in the theory of elasticity

Described below are the basic assumptions that are used in the theory of elasticity. These assumptions are common to all elastic problems.

1. Perfectly elastic material, i.e., if a body is deformed by external forces, the body will return completely to its initial shape when the external forces are removed.
2. Homogeneous, i.e., the physical properties of the entire body are the same as any small element cut out from the body.
3. Isotropic, i.e., the elastic properties of the body are the same in all directions.

3.2 Theory of bending of thin plates

The theory for thin plates is similar to the theory for beams. In pure bending of beams, "the stress distribution is obtained by assuming that cross-sections of the bar remain plane during bending and rotate only with respect to their neutral axes so as to be always normal to the deflection curve." (Timoshenko, 1936, p. 319). This is shown in the sketch below:

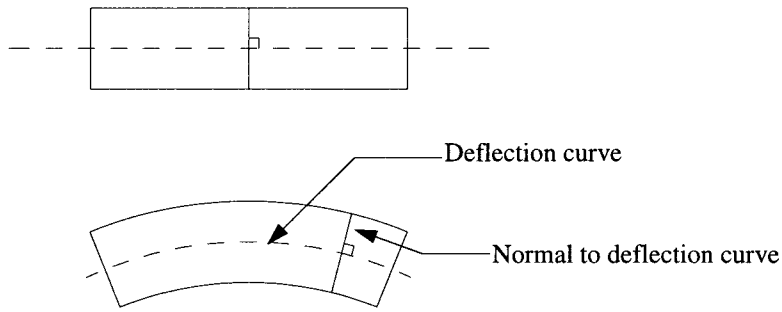

Figure 15: Beam under pure bending.

For a thin plate, bending in two perpendicular directions occur. A rectangular plate element is shown below:

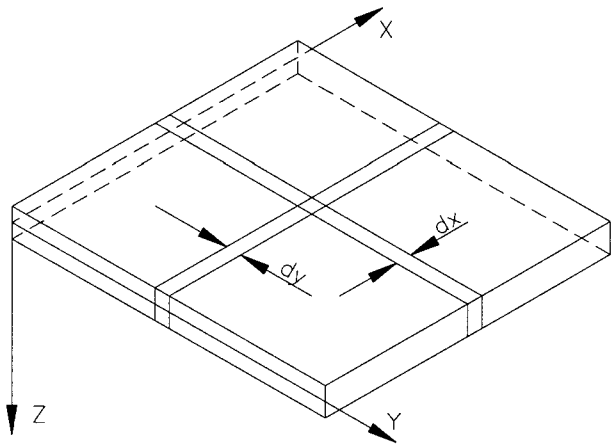

Figure 16: Thin plate notation.

Consider a small element cut out by two pairs of planes, parallel to the xz-plane and the yz-plane. This small differential element is shown below:

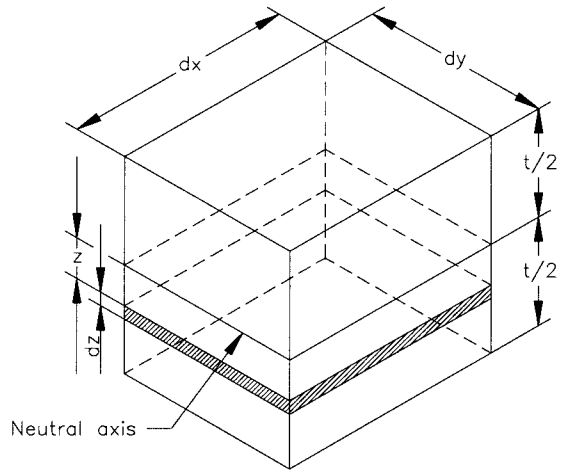

Figure 17: Differential element notation.

The basic assumptions of elastic plate bending are:

1. Perfectly flat plate and of uniform thickness

2. The thickness of the plate is small compared with other dimensions. For plate bending, the thickness, *t*, is less than or equal to 1/4 of the smallest width of the plate. For plate buckling equations, the thickness, *t*, should be 1/10 of the smallest width of the plate, (Young, 1989).

3. Deflections are small, i.e., smaller or equal to 1/2 of the thickness, (Young, 1989).

4. The middle plane of the plate does not elongate during bending and remains a neutral surface.

5. The lateral sides of the differential element, in the above figure, remain plane during bending and rotate only to be normal to the deflection surface. Therefore, the stresses and strains are proportional to their distance from the neutral surface.

6. The bending and twisting of the plate element resist the applied loads. The effect of shearing forces is neglected.

From the above assumptions the strains in a plane element, in the x- and y-directions are given by:

$$\varepsilon_x = \frac{z}{\rho_x} \qquad \varepsilon_y = \frac{z}{\rho_y} \qquad \textbf{Eq. 2}$$

where: z = distance from neutral surface

$1/\rho_x$ = curvatures of the neutral surface in a section parallel to the xz-plane

$1/\rho_y$ = curvatures of the neutral surface in a section parallel to the yz-plane

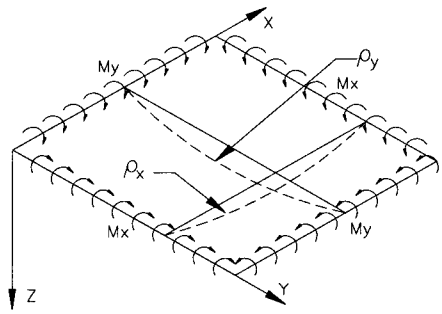

Figure 18: Curvatures of the neutral surface in a plate section.

and from Hooke's law, the strains ε_x and ε_y are related to the stresses σ_x and σ_y as follows:

$$\varepsilon_x = \frac{1}{E}\left(\sigma_x - \nu\sigma_y\right) \qquad \varepsilon_y = \frac{1}{E}\left(\sigma_y - \nu\sigma_x\right) \qquad \textbf{Eq. 3}$$

where: E = Young's modulus

σ_x = normal stresses in the x-direction

σ_y = normal stresses in the y-direction

ν = Poisson's ratio

By combining Eq. 2 and Eq. 3, and solving for the normal stresses σ_x and σ_y, yields

$$\sigma_x = \frac{Ez}{\left(1-\nu^2\right)}\left(\frac{1}{\rho_x} + \frac{\nu}{\rho_y}\right) \qquad \sigma_y = \frac{Ez}{\left(1-\nu^2\right)}\left(\frac{1}{\rho_y} + \frac{\nu}{\rho_x}\right) \qquad \textbf{Eq. 4}$$

The normal stresses above act on the lateral sides of the element in Figure 17 and can be reduced to couples, which must equal the externally applied moments. It can then be shown that, the edge moments M_x and M_y are given by:

$$M_x = D\left(\frac{1}{\rho_x} + \nu\frac{1}{\rho_y}\right) \qquad M_y = D\left(\frac{1}{\rho_y} + \nu\frac{1}{\rho_x}\right) \qquad \textbf{Eq. 5}$$

where: $D = \dfrac{Et^3}{12\left(1-\nu^2\right)}$; flexural rigidity of the plate. **Eq. 6**

This quantity corresponds to the *EI*-value of a beam of unit width. The term $(1-\nu^2)$ increases the rigidity of the plate compared to a beam of the same width. The reason for this is that moments in one direction create a curvature in a perpendicular direction, to form a so called *anticlastic* surface. The plate's resistance to this the second curvature, has the effect of an increase in the rigidity of the plate.

Let the deflection, in the z-direction, of the plate be w, then by using the approximate formulas for the curvatures of a plate, the curvatures are given by:

$$\frac{1}{\rho_x} = -\frac{\partial^2 w}{\partial x^2} \qquad \frac{1}{\rho_y} = -\frac{\partial^2 w}{\partial y^2} \qquad \textbf{Eq. 7}$$

Substituting Eq. 7 into Eq. 5 yields the following expressions for the moments:

$$M_x = -D\left(\frac{\partial^2 w}{\partial x^2} + \nu\frac{\partial^2 w}{\partial y^2}\right) \qquad M_y = -D\left(\frac{\partial^2 w}{\partial y^2} + \nu\frac{\partial^2 w}{\partial x^2}\right) \qquad \textbf{Eq. 8}$$

From basic theory of elasticity, the relationship between shear strain and shear stress is given by:

$$\gamma_{xy} = \frac{2(1+\nu)}{E} \times \tau_{xy} \qquad \textbf{Eq. 9}$$

It can then be shown that the twisting moment is given by:

$$M_{xy} = -D(1-\nu)\frac{\partial^2 w}{\partial x \partial y} \qquad \textbf{Eq. 10}$$

Consider a plate that is subjected to a distributed lateral load (as shown below), acting perpendicular to the middle plane of the plate, where $q(x, y)$ is the intensity of the load. In the general case, the intensity q is a function of x and y.

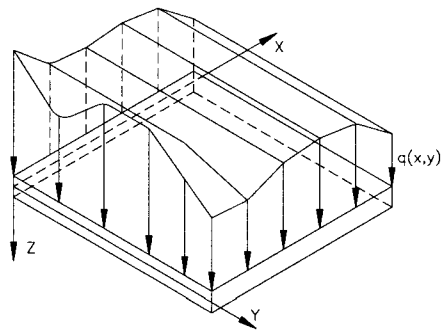

Figure 19: Distributed lateral load on a plate.

By integrating the following fourth-order partial differential equation, the deflection surface can be found:

$$\frac{\partial^4 w}{\partial x^4} + 2\frac{\partial^4 w}{\partial x^2 \partial y^2} + \frac{\partial^4 w}{\partial y^4} = \frac{q}{D} \qquad \textbf{Eq. 11}$$

If the deflection surface is known, all the stresses can be calculated. Next, the definition of the boundary conditions will be discussed.

3.3 Mathematical definitions of the boundary conditions

In order to integrate the above differential equation, the distributed load and the boundary conditions must be known. Discussed below are the mathematical definitions for a fixed (clamped or built-in) edge, simply supported edge and for a free edge.

3.3.1 Fixed Edge

Shown below is a sketch of a fixed edge:

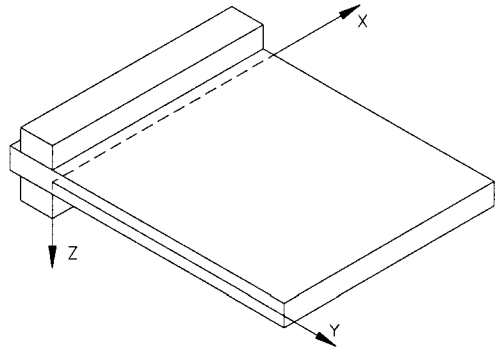

Figure 20: Fixed edge.

The deflection is zero along the fixed edge and the slope of the middle plane of the plate is zero for a fixed edge. Using the above coordinate system, the boundary conditions are:

$$(w)_{y=0} = 0 \qquad \left(\frac{\partial w}{\partial y}\right)_{y=0} = 0 \qquad \textbf{Eq. 12}$$

3.3.2 Simply Supported Edge

A simply supported edge has no deflections along the supported edge, however the rotation with respect to the x-axis is not restricted. A sketch of a simply supported edge is shown below:

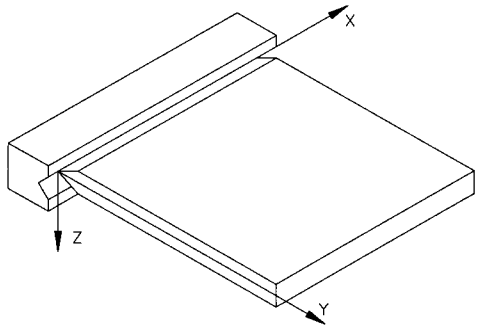

Figure 21: Simply supported edge.

Because there are no restrictions against rotation along the simply supported edge, this means that there are no bending moments along this edge. The mathematical definition of a simply supported edge is given below:

$$(w)_{y=0} = 0 \qquad \left(\frac{\partial^2 w}{\partial y^2} + \nu \frac{\partial^2 w}{\partial x^2}\right)_{y=0} = 0 \qquad \textbf{Eq. 13}$$

3.3.3 Free Edge

Along an edge that has no supports, the bending and twisting moments and the vertical shearing forces will all be zero. Let the edge $x = a$ be free in the sketch below:

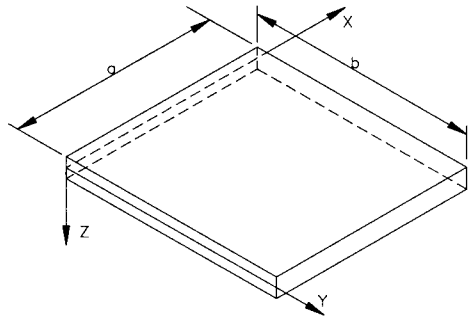

Figure 22: Free edge.

$$(M_x)_{x=a} = 0 \qquad (M_{xy})_{x=a} = 0 \qquad (Q_x)_{x=a} = 0 \qquad \textbf{Eq. 14}$$

The two boundary conditions above for the twisting moment and the shearing forces can be combined to one boundary condition, as was proved by Kirchhoff (1850), i.e.,

$$\left(Q_x - \frac{\partial M_{xy}}{\partial y}\right)_{x=a} = 0 \qquad \textbf{Eq. 15}$$

The analytical expression for the above boundary condition can be shown to be:

$$\left[\frac{\partial^3 w}{\partial x^3}+(2-\nu)\frac{\partial^3 w}{\partial x \partial y^2}\right]_{x=a}=0 \qquad \textbf{Eq. 16}$$

The expression for the requirement that the bending moment is zero can be expressed as follows:

$$\left(\frac{\partial^2 w}{\partial x^2}+\nu\frac{\partial^2 w}{\partial y^2}\right)_{x=a}=0 \qquad \textbf{Eq. 17}$$

3.4 Plate subjected to in-plane loads

If a plate has, in addition to the distributed lateral load, forces that are applied in the middle plane of the plate, the effect on plate bending can be considerable. The differential equation for the deflection surface can then be shown to be (Saint Venant derived this differential equation in 1883):

$$\frac{\partial^4 w}{\partial x^4}+2\frac{\partial^4 w}{\partial x^2 \partial y^2}+\frac{\partial^4 w}{\partial y^4}=\frac{1}{D}\left(q+N_x\frac{\partial^2 w}{\partial x^2}+2N_{xy}\frac{\partial^2 w}{\partial x \partial y}+N_y\frac{\partial^2 w}{\partial y^2}\right) \qquad \textbf{Eq. 18}$$

where: q = distributed lateral load intensity

N_x = edge force per unit length in the x-direction

N_y = edge force per unit length in the y-direction

N_{xy} = edge shearing force per unit length

The above differential equation is not valid for large deflections, i.e., when the middle plane of the plate stretches. This would be the case when inelastic buckling occurs and/or when the plate carries ultimate load.

4. ELASTIC STABILITY OF THIN PLATES

The analytical solution of elastic instability problems can be done by integration of the differential equation of the deflected shape of the buckled plate or by the energy method. The energy method can be used when an analytical solution of Eq. 17 can not be found. However, in order to use the energy method a good approximation of the deflected shape of the plate needs to be known.

4.1 Integration of differential equation of equilibrium

A brief description of how to solve for the critical buckling load will be done next. One way of analyzing a plate for critical buckling load is to assume that the plate will buckle slightly under edge compression. Then the magnitude of this edge compression to keep the plate in this slightly buckled shape is the critical buckling load. Consider a simply supported thin flat plate with a uniform compressive load acting in the middle plane, as shown below:

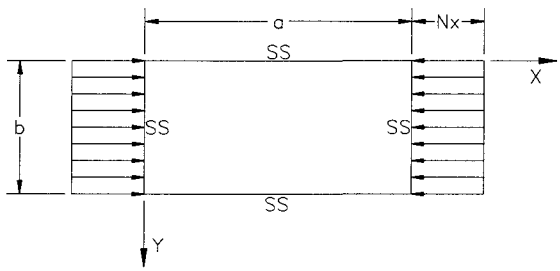

Figure 23: Simply supported flat plate subjected to uniform compression.

The differential equation of the buckled shape is obtained from Eq. 17, and by setting q = 0 (i.e., there are no lateral loads), $N_x = \sigma t$, $N_y = 0$, $N_{xy} = 0$ and if no body forces are present, the differential equation of the buckled plate then becomes:

$$\frac{\partial^4 w}{\partial x^4} + 2\frac{\partial^4 w}{\partial x^2 \partial y^2} + \frac{\partial^4 w}{\partial y^4} = \frac{1}{D}\left(\sigma t \frac{\partial^2 w}{\partial x^2}\right) \qquad \textbf{Eq. 19}$$

where: σ = compressive stress

t = thickness of plate

Assuming that the plate buckles in m sinusoidal half-waves in the direction of the compressive load, the solution is then assumed to be in the form,

$$w = f(y) \times \sin\frac{m\pi x}{a} \qquad \textbf{Eq. 20}$$

where $f(y)$ is a function of y only. This expression needs to satisfy the four boundary conditions that are given by:

$$(w = 0)_{x=0,a} \qquad \text{and} \qquad \left(\frac{\partial^2 w}{\partial x^2} + \nu\frac{\partial^2 w}{\partial y^2} = 0\right)_{x=0,a} \qquad \textbf{Eq. 21}$$

By substituting Eq. 20 in Eq. 19, the following differential equation is obtained:

$$\frac{d^4 f}{dy^4} - \frac{2m^2\pi^2}{a^2}\frac{d^2 f}{dy^2} + \left(\frac{m^4\pi^4}{a^4} - \frac{\sigma t}{D}\frac{m^2\pi^2}{a^2}\right)f = 0 \qquad \textbf{Eq. 22}$$

The general solution is given by:

$$f(y) = A_1\cosh(\alpha y) + A_2\sinh(\alpha y) + A_3\cos(\beta y) + A_4\sin(\beta y) \qquad \textbf{Eq. 23}$$

where:
$$\alpha = \left[\frac{m^2\pi^2}{a^2} + \sqrt{\frac{\sigma t}{D}\frac{m^2\pi^2}{a^2}}\right]^{1/2} \qquad \textbf{Eq. 24}$$

$$\beta = \left[-\frac{m^2\pi^2}{a^2} + \sqrt{\frac{\sigma t}{D}\frac{m^2\pi^2}{a^2}}\right]^{1/2} \qquad \textbf{Eq. 25}$$

The constants of integration above, are determined by using the given boundary conditions. Four equations can then be found involving A_1 through A_4. These four equations can be written in matrix form as shown below:

$$\begin{bmatrix} 1 & 0 & 1 & 0 \\ \cosh(\alpha b) & \sinh(\alpha b) & \cos(\beta b) & \sin(\beta b) \\ \gamma^2 & 0 & -\delta^2 & 0 \\ \gamma^2\cosh(\alpha b) & \gamma^2\sinh(\alpha b) & -\delta^2\cos(\beta b) & -\delta^2\sin(\beta b) \end{bmatrix} \begin{Bmatrix} A_1 \\ A_2 \\ A_3 \\ A_4 \end{Bmatrix} = 0 \qquad \textbf{Eq. 26}$$

where: $\gamma^2 = \alpha^2 - \nu\frac{m^2\pi^2}{a^2}$ **Eq. 27**

$\delta^2 = \beta^2 + \nu\frac{m^2\pi^2}{a^2}$ **Eq. 28**

The above four equations are satisfied if all four constants of integration equal zero, i.e., a trivial solution and that $w = 0$, and that would be the unbuckled shape of the plate. For a non-trivial solution to exist, the determinant of the above matrix must equal zero, as shown below:

$$-\left(\gamma^2 + \delta^2\right)^2 \sinh(\alpha b)\sin(\beta b) = 0 \quad \textbf{Eq. 29}$$

This equation is the characteristic equation and defines the stability of the plate. Defining the following parameters:

$$K = \frac{\sigma t b^2}{\pi^2 D} \quad \text{and} \quad \phi = \frac{a}{b} \quad \textbf{Eq. 30}$$

If the above parameters K and ϕ are substituted into Eq. 24 and Eq. 25, it can be shown that

$$\alpha b = \left[\frac{m\pi^2}{\phi^2}\left(\sqrt{K} + \frac{m}{\phi}\right)\right]^{1/2} \quad \textbf{Eq. 31}$$

$$\beta b = \left[\frac{m\pi^2}{\phi^2}\left(\sqrt{K} - \frac{m}{\phi}\right)\right]^{1/2} \quad \textbf{Eq. 32}$$

Denoting αb and βb with p and q and $\gamma^2 b^2$ and $\delta^2 b^2$ with r and s, it can be shown that,

$$\left(r^2 + s^2\right) = \left(p^2 + q^2\right) = \frac{2m^2\pi^2}{\phi^2}\sqrt{K} \quad \textbf{Eq. 33}$$

The solution to the characteristic equation can then be written as a function of K and ϕ. Setting $m = 1$, i.e., the buckled plate has only one-half wave in the direction of the compressive load. For this particular example, a plate simply supported on all four edges, the relationship between K and ϕ is given by:

$$K = \frac{1}{\phi^2} + \phi^2 + 2 \qquad \textbf{Eq. 34}$$

This function is shown below:

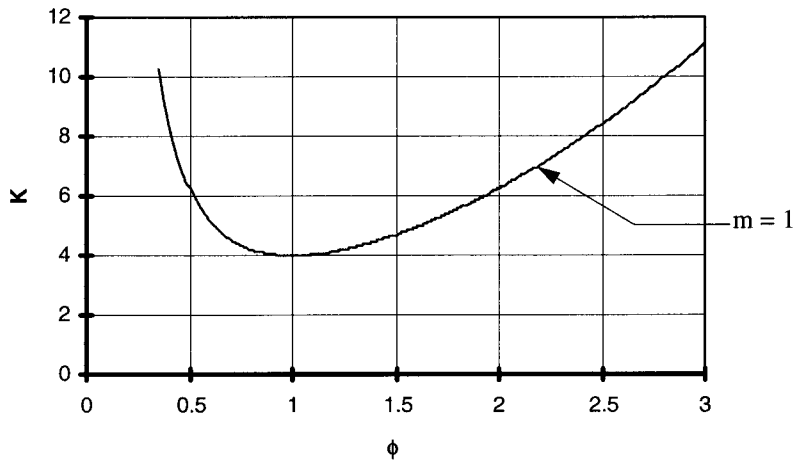

Figure 24: Buckling coefficient, K versus aspect ratio, ϕ.

As can be seen from the above graph, the function has a minimum at $\phi = 1$ which corresponds to $K = 4$. Rewriting Eq. 30,

$$\sigma = \frac{K\pi^2 D}{tb^2} = \frac{K\pi^2 E}{12(1-\nu^2)}\left(\frac{t}{b}\right)^2 \qquad \textbf{Eq. 35}$$

The above expression is the well-known equation for the critical buckling stress, and K is the buckling coefficient.

Timoshenko (1961) showed that the deflection surface of a buckled simply supported plate is a double sine curve, and can be represented by the following equation:

$$w = \sum_{m=1}^{\infty}\sum_{n=1}^{\infty} a_{mn} \sin\frac{m\pi x}{a} \sin\frac{n\pi y}{b} \qquad \textbf{Eq. 36}$$

4.2 The energy method

As stated earlier, the energy method can also be used to find the critical buckling load. The energy method has the advantage of finding the critical load in a direct and simple way, and for cases where it is not possible to find an analytical solution to the differential equation of the deflected shape of the buckled plate. The principle of conservation of energy states that the strain energy stored in a system is equal to the work done by the applied loads. If the work done by the applied loads becomes larger than the strain energy due to bending (for any shape of the deflection surface) buckling occurs. However, a good approximation of the shape of the deflection surface of the buckled plate needs to be known. For cases with partial boundary conditions, the energy method has been used to find critical buckling stresses. Hamada et. al. (1967) and Norris et. al. (1951) used the energy method to analyze cases with partial boundary conditions, as was described in the literature review section. A very brief description of the energy method will be done next.

Consider a flat plate subjected to loads acting in the middle plane of the plate. A small amount of lateral bending is produced, which is consistent with the given boundary conditions. If no stretching of the middle plane occurs, the energy of bending and the work done by the applied loads in the middle plane only need to be considered. Then, the critical forces can be found from,

$$\Delta T_1 = \Delta U \qquad \textbf{Eq. 37}$$

where: ΔT_1 = work done by external forces
ΔU = strain energy of bending

The buckled shape of a simply supported plate was given from Eq. 36, as follows:

$$w = \sum_{m=1}^{\infty}\sum_{n=1}^{\infty} a_{mn} \sin\frac{m\pi x}{a} \sin\frac{n\pi y}{b}$$

The strain energy of bending can then be shown to be:

$$\Delta U = \frac{\pi^4 ab}{8} D \sum_{m=1}^{\infty}\sum_{n=1}^{\infty} a_{mn}\left(\frac{m^2}{a^2}+\frac{n^2}{b^2}\right)^2 \qquad \textbf{Eq. 38}$$

Work done by the externally applied compressive forces, can be shown to be:

$$\Delta T_1 = \frac{\pi^2 b}{8a} N_x \sum_{m=1}^{\infty}\sum_{n=1}^{\infty} m^2 a_{mn}^2 \qquad \textbf{Eq. 39}$$

Critical values of the compressive forces can then be found by equating Eq. 38 and Eq. 39,

$$\frac{\pi^2 b}{8a} N_x \sum_{m=1}^{\infty}\sum_{n=1}^{\infty} m^2 a_{mn}^2 = \frac{\pi^4 ab}{8} D \sum_{m=1}^{\infty}\sum_{n=1}^{\infty} a_{mn}\left(\frac{m^2}{a^2}+\frac{n^2}{b^2}\right)^2$$

and solving for N_x:

$$N_x = \frac{\pi^2 a^2 D \sum_{m=1}^{\infty}\sum_{n=1}^{\infty} a_{mn}^2\left(\frac{m^2}{a^2}+\frac{n^2}{b^2}\right)^2}{\sum_{m=1}^{\infty}\sum_{n=1}^{\infty} m^2 a_{mn}^2} \qquad \textbf{Eq. 40}$$

It can then be shown that Eq. 40 becomes a minimum if all the coefficients a_{mn}, except one, are set to zero. Eq. 40 then becomes:

$$N_x = \frac{\pi^2 a^2 D}{m^2}\left(\frac{m^2}{a^2}+\frac{n^2}{b^2}\right)^2 \qquad \textbf{Eq. 41}$$

By setting $n = 1$, N_x will be a minimum. This means that the plate buckles so there is just one-half wave in the perpendicular direction and many half-waves in the direction of the applied loads. The expression for the critical load then becomes:

$$\left(N_x\right)_{cr} = \frac{\pi^2 D}{a^2}\left(m + \frac{1}{m}\frac{a^2}{b^2}\right)^2 \qquad \textbf{Eq. 42}$$

5. FINITE ELEMENT ANALYSIS

There are two parts to the finite element analysis (FEA). First, the linear elastic buckling load was obtained by using a linear eigenvalue buckling analysis program. Verification of the results obtained from the FEA was done as follows: A flat plate with known linear elastic buckling stress was modeled using the FEA program. The linear elastic buckling stress obtained from the FEA program was then compared to a closed-form solution. Several models with increasingly more and more elements were analyzed until the FEA solution was within 5% of the closed-form solution.

The second part of the finite element analysis was to estimate the ultimate strength of the plate. The ultimate strength of the plate was obtained as follows: A non-linear finite element analysis procedure was selected. In the non-linear finite element method initial imperfections and elasto-plastic conditions could be modeled. The first buckled mode shape obtained from the linear elastic solver was used as an initial imperfection. By doing this the worst case scenario would be modeled, i.e., a flat plate with an initial imperfection corresponding to the first buckled mode shape. Von Mises yield condition was used in the analysis, with a tangent modulus of zero. By choosing a tangent modulus of zero, again, a worst case is modeled. An incremental solution procedure was then used in the non-linear FEA. The ultimate strength of the flat plate was found when a small increase in the load resulted in a very large deflection of the plate, i.e., the stiffness of the plate approached zero. The non-linear finite element method was compared to an approximate method, the "effective-width" method.

5.1 Linear elastic buckling strength

The linear elastic buckling load was obtained by using a commercially available FEA-program, the ALGOR-software, (Algor, Inc.; 150 Beta Drive; Pittsburgh, Pa 15238). This program determines the load which brings the structure to the bifurcation point. The predicted buckling load is the Euler buckling load. The bifurcation point is defined as follows (Galambos, 1988): At the bifurcation point, the compressed member can be in equilibrium in two different configurations. The member can either be straight or in a slightly deflected shape. If a plot of axial load versus lateral deflection is made, a branch

point occurs at the bifurcation point. After the bifurcation point two different load/deflection curves are mathematically valid. Idealized load-displacement paths are shown in Figure 25 below.

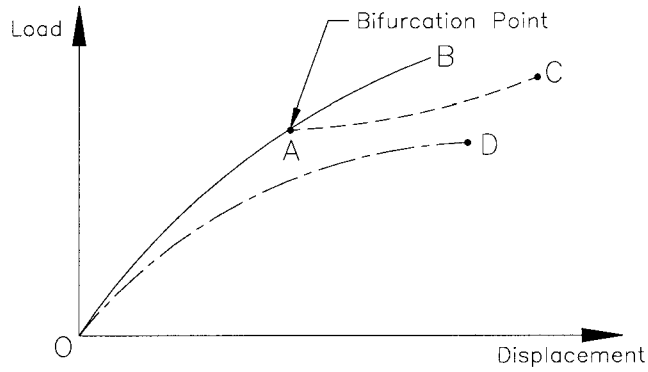

Figure 25: Idealized load-displacement paths.

The solid line represents a perfect structure and displaces along a basic path (OAB) and the bifurcation occurs at point A. The dashed line AC represents the post-buckling path, and this path can either rise or descend depending on what type of structure and loading is considered. The third line (OD), applies to structures with initial imperfections and as can be seen a bifurcation point does not exist.

The basic equation to be solved in finite element analysis is

$$\{F\} = [K]\{d\} \qquad \textbf{Eq. 43}$$

where: F = global nodal force vector

K = global stiffness matrix

d = global nodal displacement vector

By using the minimum potential energy principle the total potential energy of a plate element can be written as (Allen, 1980):

$$V_e = \frac{1}{2}\{\delta\}^T[K_L + K_G]\{\delta\} \qquad \textbf{Eq. 44}$$

where: V_e = total potential energy of the plate element

δ = nodal displacement vector

K_L = linear stiffness matrix

K_G = geometric stiffness matrix

At the critical load, the total potential energy is a minimum and the homogeneous equation

$$[K_L + K_G]\{\delta\} = 0 \qquad \textbf{Eq. 45}$$

has a non-trivial solution. The critical stress is then the smallest root of the determinant of the following equation:

$$\det(K_L + \lambda_{cr} K_G) = 0 \qquad \textbf{Eq. 46}$$

where: λ_{cr} = the buckling load factor

As was the case in the theoretical development of the critical buckling load, the FEA-model of the flat plate is assumed to be perfectly flat and entirely elastic, i.e., the buckling takes place in the elastic region. The linear elastic buckling load was found for the flat plate shown below with non-continuous boundary conditions. The plate is subjected to uniform compression and has one partially supported unloaded edge.

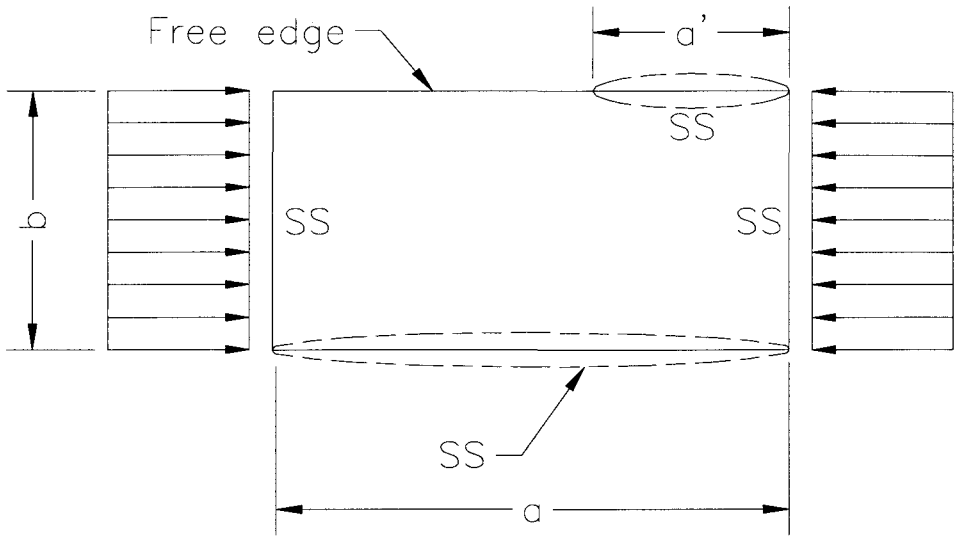

Figure 26: Flat plate under uniform compression with a partially supported unloaded edge.

where: a = length of the plate

b = width of the plate

a' = supported length of an unloaded, longitudinal edge

SS = simply supported edge

Four aspect ratios, *a/b* were investigated for the above case: *a/b* = 1.0, 1.4, 2.0, 3.0. Dimensions and material properties for the four different plate models are given below:

a/b (--)	**Length, a (in)**	**Width, b (in)**	**Thickness, t (in)**	**Young's modulus (psi)**	**Poisson's ratio (--)**
1.0	2.00	2.00	0.05	30E6	0.30
1.4	2.80	2.00	0.05	30E6	0.30
2.0	4.00	2.00	0.05	30E6	0.30
3.0	6.00	2.00	0.05	30E6	0.30

The supported length on the partially supported edge was varied between zero and the plate length, i.e., $0 \leq a'/a \leq 1$, where *a'* is the length of the support on the partially

supported edge. Two closed-form solutions are known for each set of plates, namely when the top edge (in Figure 26) is supported along the entire edge and when the edge is free. The finite element solution should, therefore, correspond to the closed-form solutions at these points. One verification of the FEA-model and the corresponding buckling load can therefore be done by considering these two cases.

The linear elastic buckling strength was obtained by using a linear eigenvalue solver (ALGOR-software). In the next section, the finite element models will be described showing elements used, boundary conditions and applied loads.

5.2 Description of the finite element models

Shown in Figure 27 is a sketch of the finite element model used in the linear elastic buckling model. Boundary conditions are as follows: Translational boundary conditions are denoted by T_x, T_y, T_z, where the subscript denotes along what axis the translational boundary constraint is applied.

In this work, the FEA-results are compared to closed-form solutions, therefore, the boundary conditions used in the FEA-model must correspond to boundary conditions used in the analytical solutions. In Figure 26 above, the boundary conditions are given as simply supported along the edges. From Eq. 12 in the theory section, the mathematical definition of a simple support was given as:

$$(w)_{y=0} = 0 \quad \text{and} \quad \left(\frac{\partial^2 w}{\partial y^2} + \nu \frac{\partial^2 w}{\partial x^2}\right)_{y=0} = 0$$

The first equation states that there are no deflections along the supported edges, and the second equation indicates that there are no bending moments along the supported edges. Translational boundary conditions must therefore be used in the FEA-model. Referring to Figure 27, on the left edge, boundary conditions T_x and T_y are applied along the edge. Translations are therefore restricted in the x-and y-directions, where the x-direction is the out of plane direction and the y-direction is the longitudinal direction. On the bottom edge, the boundary conditions T_x and T_z are applied which constrains the translation in the transverse direction, (z-direction) and in the x-direction. The right and top edge only have

the out-of-plane boundary condition, T_x. With these boundary conditions, there are no deflections in the x-direction along the edges and the plate can still contract in the y-and z-directions, also, no rotational restrictions are imposed on the plate model. Similar boundary conditions will be used for the non-linear FEA-model. The applied load was distributed evenly along the one edge of the plate. At the two corner nodes one half the nodal load was applied, as shown below:

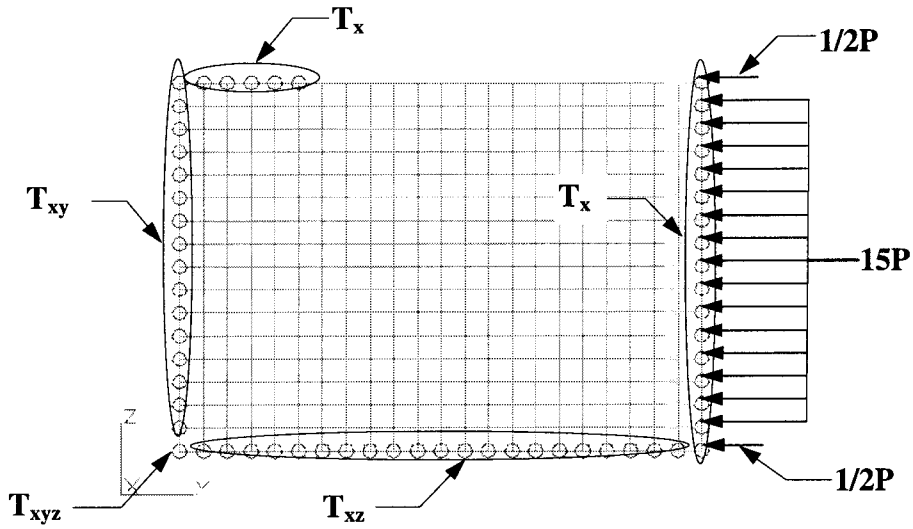

Figure 27: FEA model of partially supported plate.

A three-dimensional, isotropic, membrane plus bending linear plate element was used in this work with a Veubeke formulation (QM5 plane stress element). As stated earlier, the linear eigenvalue buckling solver finds the critical buckling load and the first buckling mode shape. In the next sections, results are presented for the four different types of plates that were investigated in this work.

5.2.1 Flat plate with aspect ratio, a/b = 1.0

Shown below is a chart for the critical buckling coefficient, K' for the case of a flat plate with an aspect ratio, *a/b* of 1.0. The x-axis shows the ratio between supported length, *a'*, and length of the plate, *a,* for the unloaded edges and the critical buckling coefficients are plotted against the y-axis.

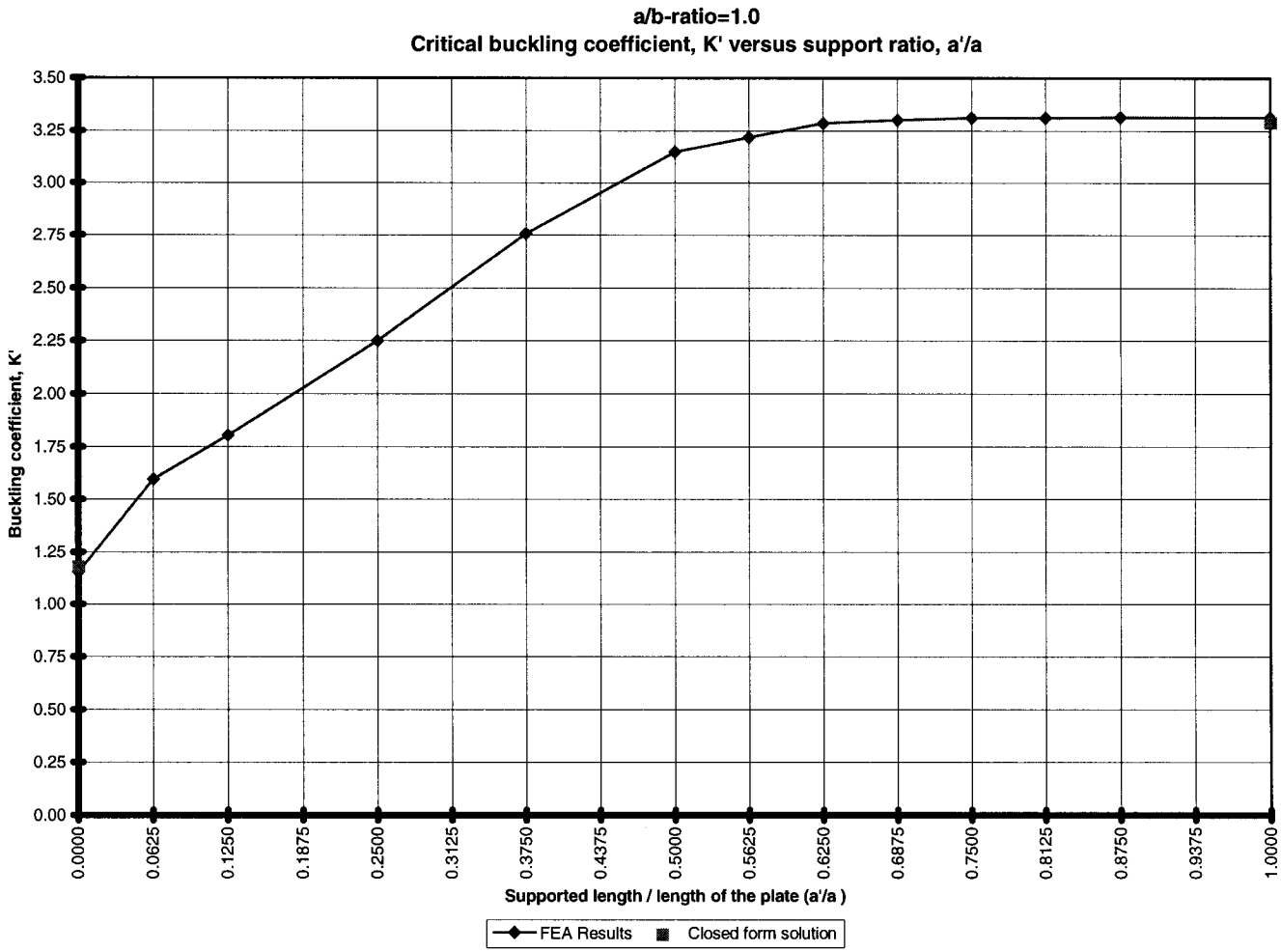

Figure 28: Buckling coefficient, K' for a flat plate with a/b=1.0.

From the above chart it is interesting to note that the critical buckling coefficient does not decrease dramatically until the unsupported length is greater than the supported length. A comparison between the FEA and closed-form solutions when *a'/a = 0* (free edge) and *a'/a = 1* (simply supported all around) is presented below.

Critical Buckling Coefficient, K':			
Support condition:	**Closed-form solution:**	**FEA:**	**% difference**
a'/a = 0, (One free edge)	1.18	1.16	-1.69 %
a'/a = 1, (SS)	3.29	3.31	0.608 %

As can be seen from the above results, the FEA-results correspond well with the two closed-form solutions that are available. Shown below are pictures of the buckled mode shapes for the plate with aspect ratio equal to one.

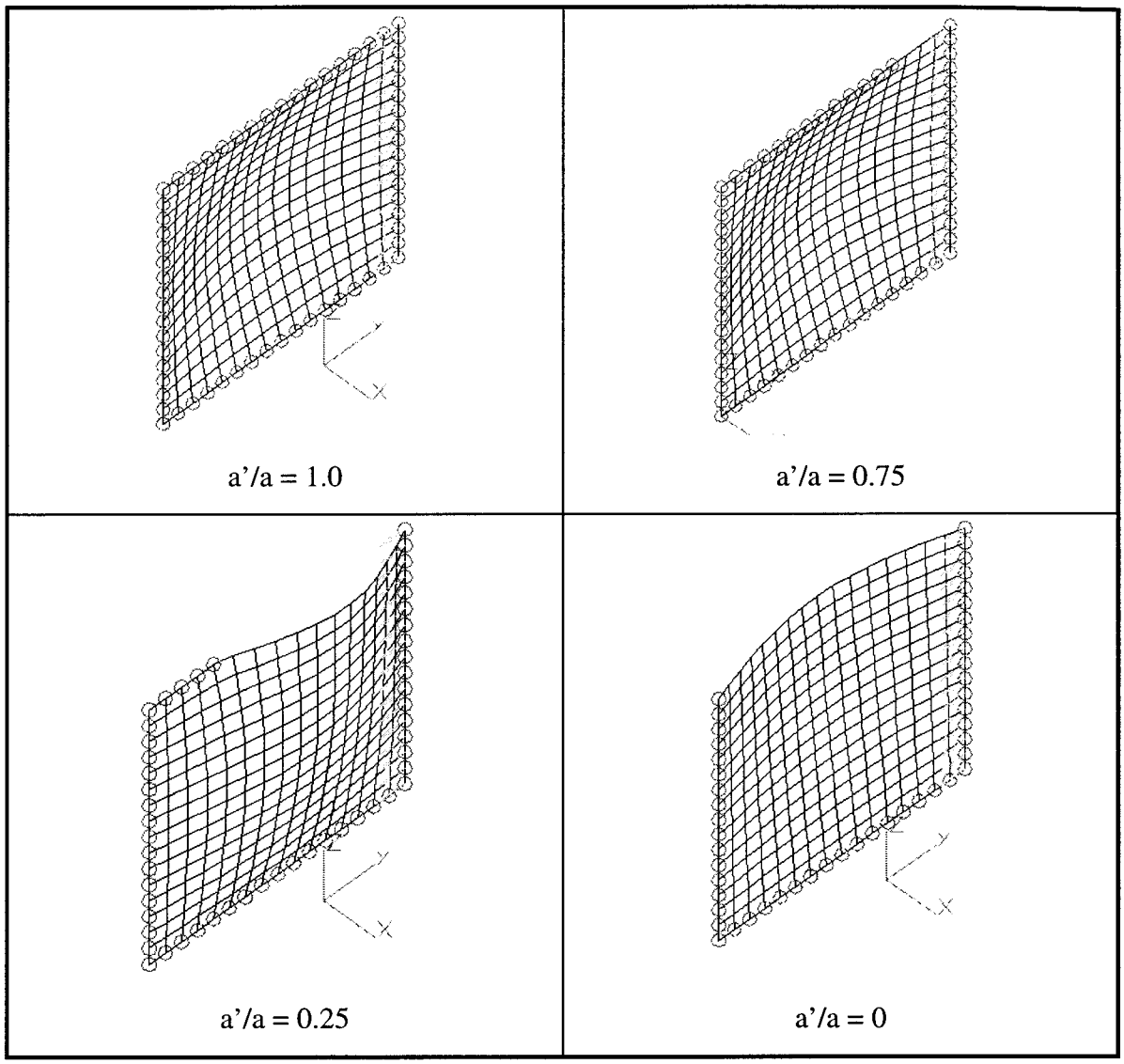

Figure 29: Buckled mode shape of plates with a/b-ratio = 1.0

5.2.2 Flat plate with aspect ratio, a/b = 1.4

The chart for the critical buckling coefficient, K' for the case of a flat plate with an aspect ratio, *a/b* of 1.4 is shown below:

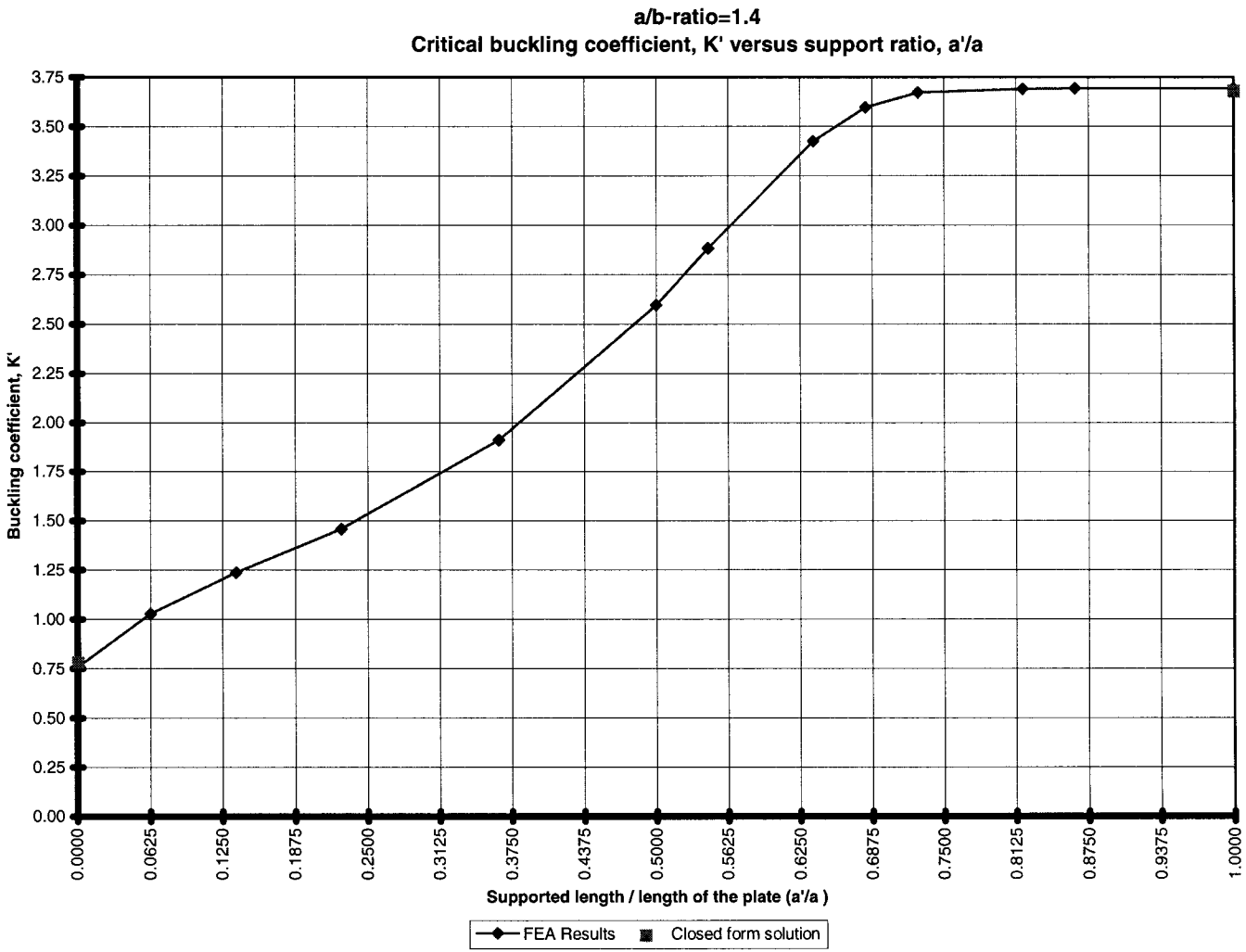

Figure 30: Buckling coefficient, K' for a flat plate with a/b=1.4.

For this case, the critical buckling coefficient starts to decrease earlier than for the plate with aspect ratio equal to one. The buckling coefficient drops when the ratio a'/a ≈ 11/16. The comparison between the FEA-results when *a'/a = 0* (free edge) and *a'/a = 1* (simply supported all around) and the closed-form solutions are presented below.

Critical Buckling Coefficient, K':			
Support condition:	**Closed-form solution:**	**FEA:**	**% difference**
a'/a = 0,(Free edge)	0.784	0.759	-3.19 %
a'/a = 1,(SS)	3.68	3.69	0.272 %

Again, the FEA-results correspond well with the closed-form solutions. The buckled mode shapes for the plates with aspect ratio equal to 1.4 are shown below:

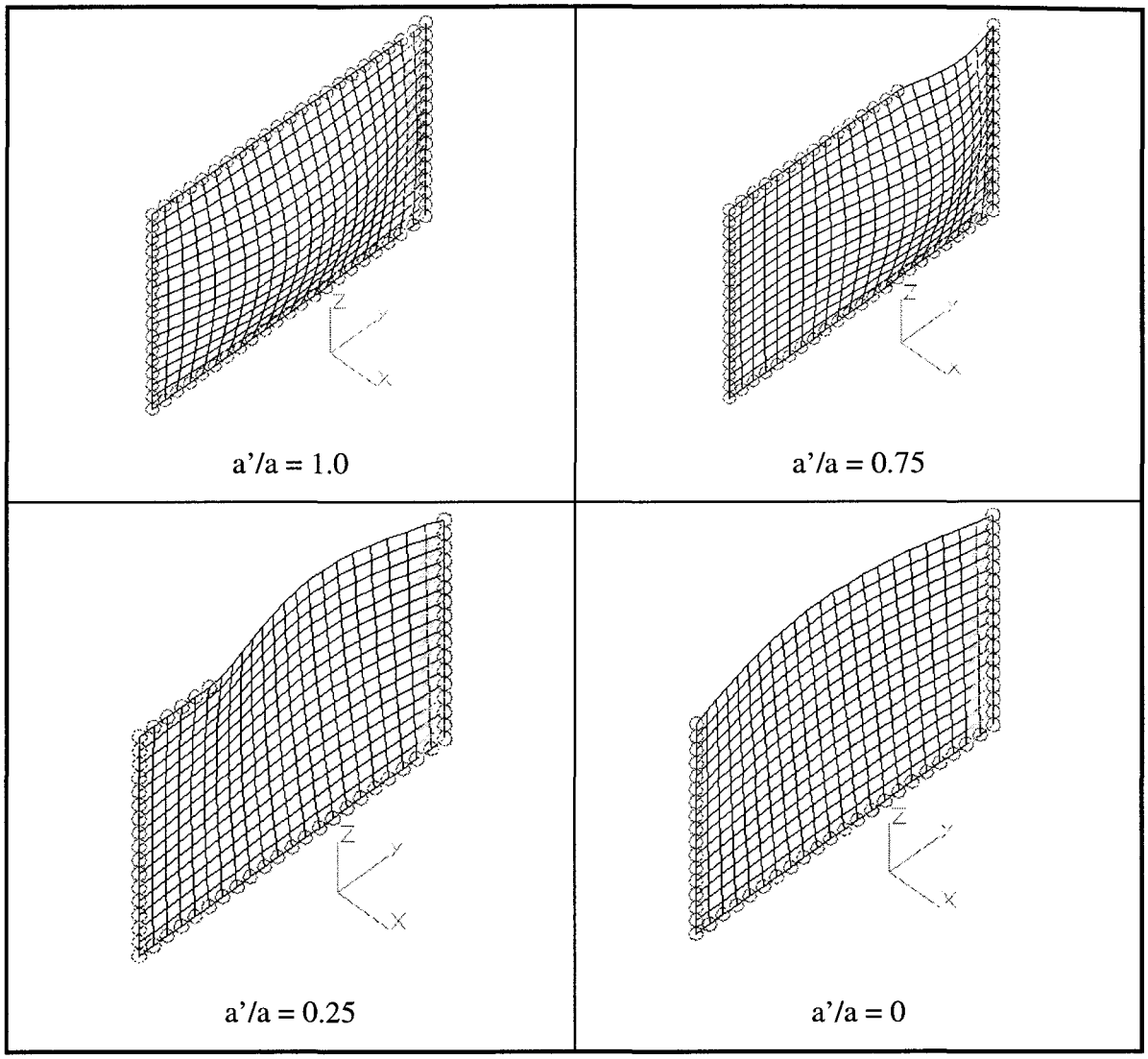

Figure 31: Buckled mode shape of plates with a/b-ratio = 1.4

5.2.3 Flat plate with aspect ratio, a/b = 2.0

The chart for the critical buckling coefficient, K' for the case of a flat plate with an aspect ratio, *a/b* of 2.0 is shown below:

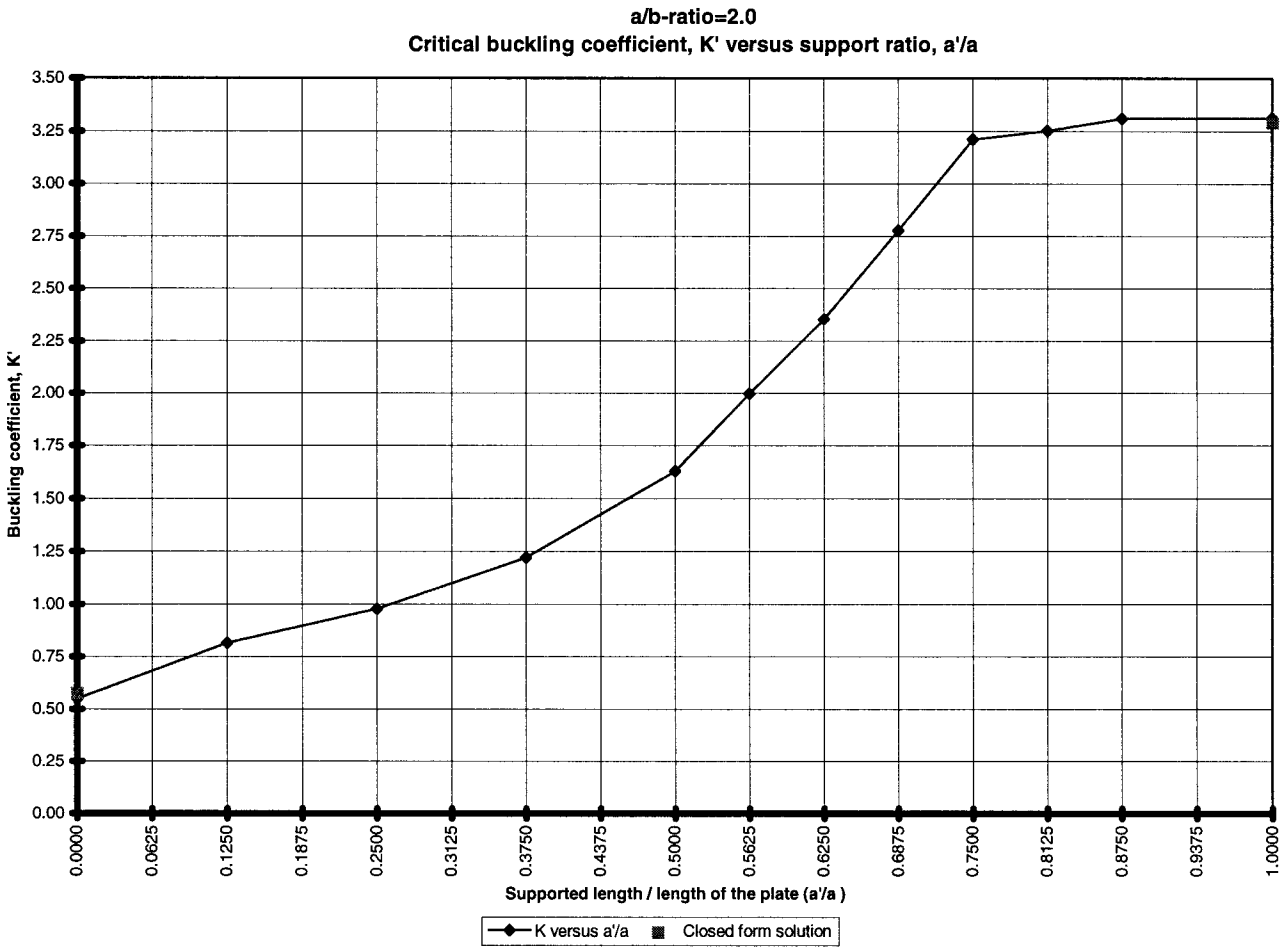

Figure 32: Buckling coefficient, K' for a flat plate with a/b=2.0.

For the aspect ratio of two, the supported length has to be approximately 75% of the length of the plate for the plate to have equivalent stiffness compared to a plate with all edges simply supported. The comparison between the FEA-results when *a'/a = 0* (free edge) and *a'/a = 1* (simply supported all around) and the closed-form solutions are presented below.

Critical Buckling Coefficient, K':			
Support condition:	**Closed-form solution:**	**FEA:**	**% difference**
a'/a = 0, Free edge	0.574	0.549	-4.36 %
a'/a = 1, SS	3.29	3.31	0.608 %

Again, the FEA-results correspond well with the closed-form solutions. The buckled mode shapes for the plates with aspect ratio equal to 2.0 are shown below:

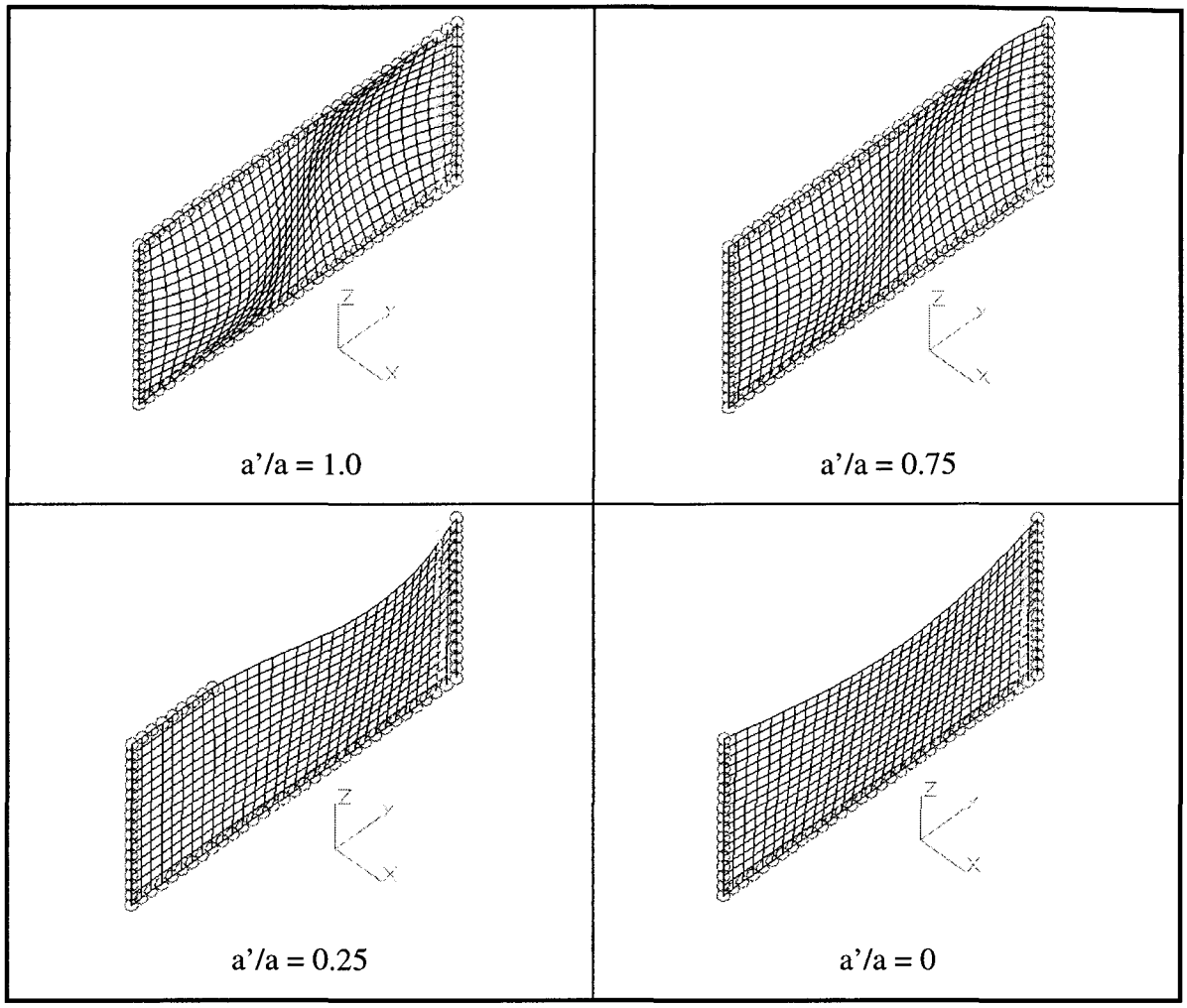

Figure 33: Buckled mode shape of plates with a/b-ratio = 2.0

5.2.4 Flat plate with aspect ratio, a/b = 3.0

The chart for the critical buckling coefficient, K' for the case of a flat plate with an aspect ratio, *a/b* of 3.0 is shown below:

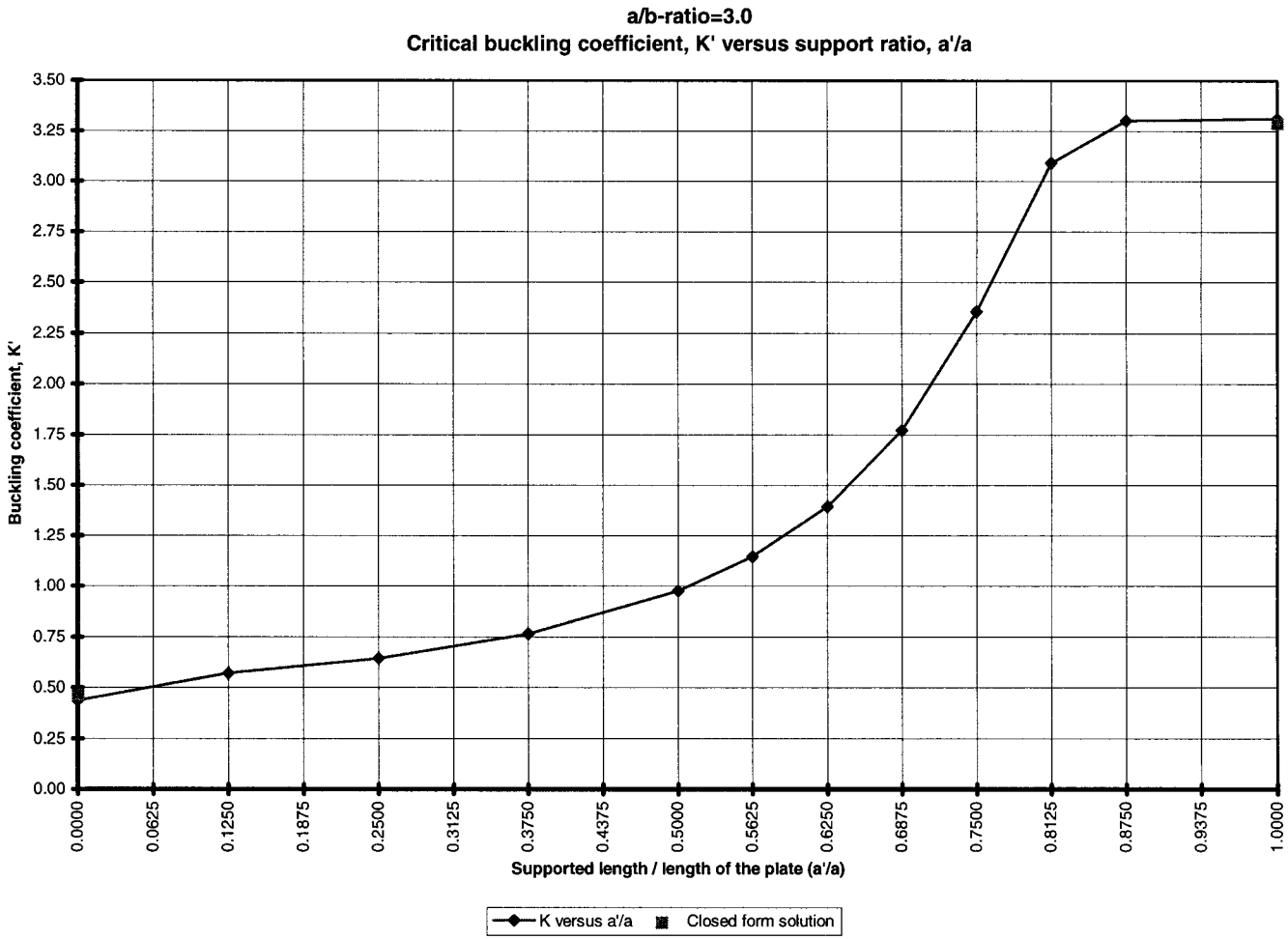

Figure 34: Buckling coefficient, K' for a flat plate with a/b=3.0.

When the supported length is less than 7/8 of the plate length, the critical buckling coefficient drops dramatically. The comparison between the FEA-results when $a'/a = 0$ (free edge) and $a'/a = 1$ (simply supported all around) and the closed-form solutions are presented below.

Critical Buckling Coefficient, *K'*:			
Support condition:	**Closed-form solution:**	**FEA:**	**% difference**
a'/a = 0, Free edge	0.464	0.438	-5.60 %
a'/a = 1, SS	3.29	3.31	0.608 %

Again, the FEA-results correspond well with the closed-form solutions. The buckled mode shapes for the plates with aspect ratio equal to 3.0 are shown below:

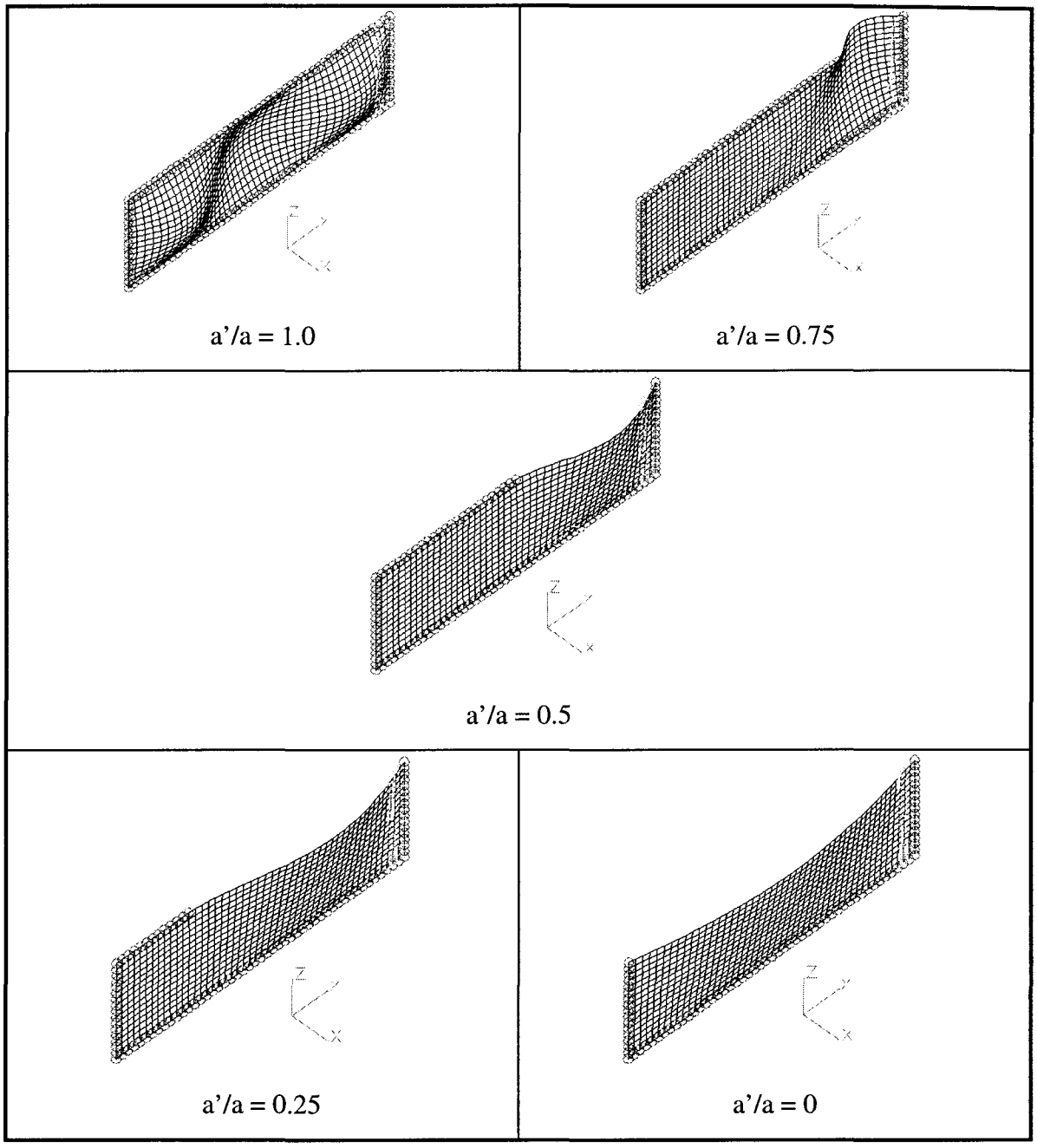

Figure 35: Buckled mode shape of plates with a/b-ratio = 3.0

In the next section, a comparison of the results obtained from the FEA is done with closed-form solutions.

5.3 Verification of the FEA-models

Closed-form solutions for the critical buckling stress exists when boundary support conditions are continuous. However, closed-form solutions are not available, to this author's knowledge, for the cases presented in this work, i.e., plates with partially supported edges. An approximate method to verify the results for the cases where closed-form solutions do not exist will be presented next. The plate will be divided into two smaller segments (see Figure 36), and these two smaller plate segments will then have continuous support boundary conditions all around.

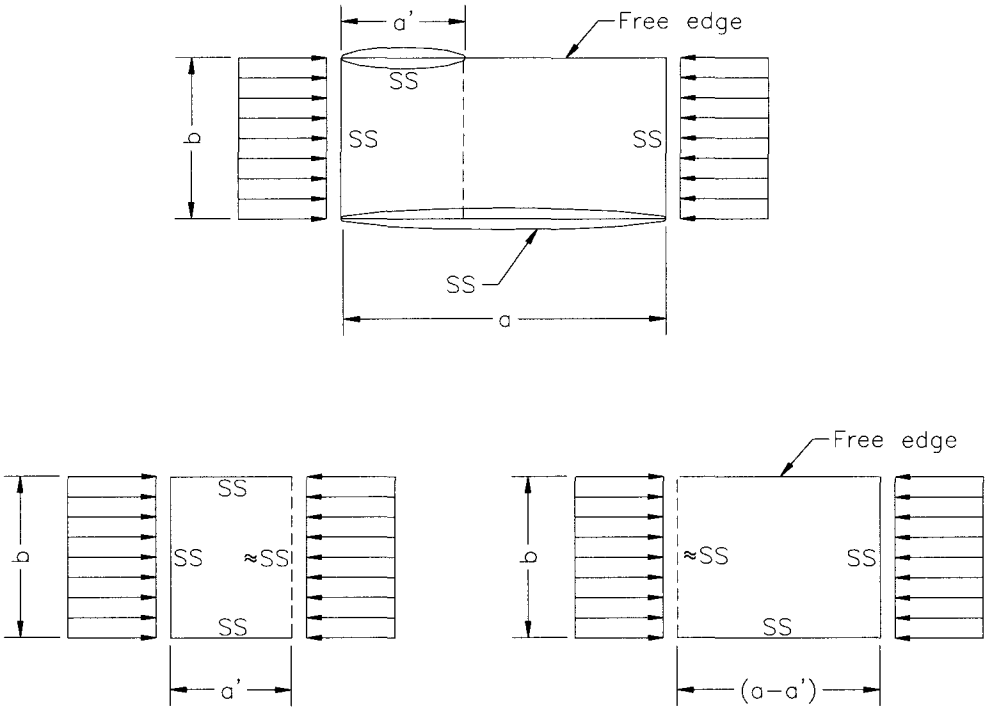

Figure 36: Plate under uniform compression divided into two segments.

The intersection between the two segments will be treated as a simple support in this work. However, the true boundary condition at the intersection is something in-between a fixed support and a simple support, as indicated in the sketch above. The intersection will carry a moment in reality, i.e., the plate will be stiffer than if it were a simple support and by treating the intersection as a simple support a worst case scenario is modeled. The buckling stress and the buckling coefficient will therefore be on the conservative side. By

modeling the two segments as described above, existing closed-form solutions can be used and critical buckling coefficients can be obtained.

The buckling coefficients obtained previously in this work, using FEA, will be compared to approximate buckling coefficients obtained by using the modeling technique described above and existing closed-form solutions. A sketch of the plate with aspect ratio 1.0 and a'/a = 0.25 is shown below:

where: a' = supported length of a longitudinal edge of the plate

a = length of the plate

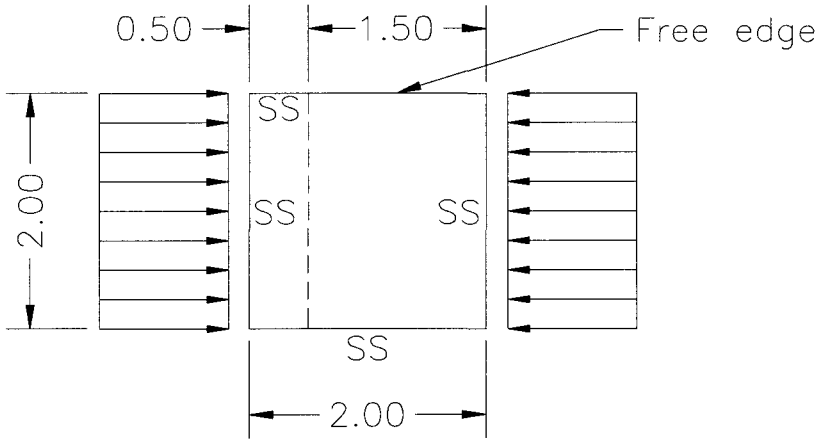

Figure 37: Plate with aspect ratio 1.0 and a'/a = 0.25

The critical buckling coefficient for the plate segment with one free edge will be found. The aspect ratio for that segment is,

$$\frac{1.50}{2.00} = 0.75$$

The critical buckling coefficient is then (Young, 1989),

$$K' = 1.88$$

Similar analysis can be done for the plates with aspect ratios 1.4, 2.0 and 3.0. A summary of the results are shown in the table below.

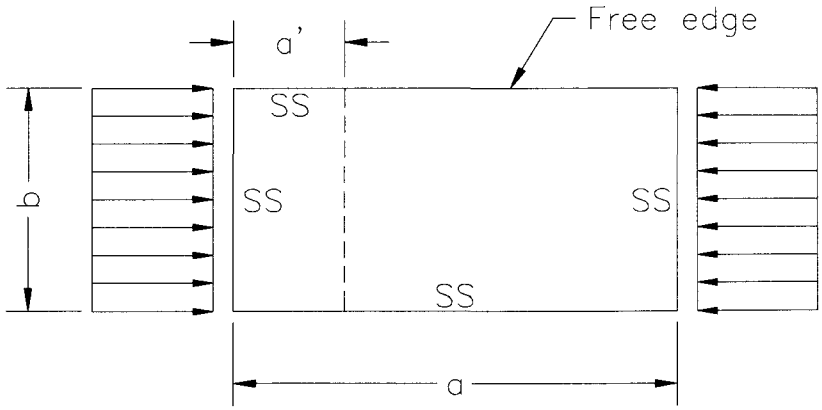

Figure 38: Flat plate with a'/a = 0.25

Comparison of critical buckling coefficients for plates with a'/a = 0.25			
a/b:	FEA:	Theory:	Percent diff.:
1.0	2.25	1.88	-16.4%
1.4	1.50	1.10	-26.7%
2.0	1.00	0.73	-27.0%
3.0	0.70	0.535	-23.9%

As was mentioned earlier, by treating the intersection between the two plate segments as a simple support the stiffness of the plate would decrease. As can be seen from the above results, the FEA predicts a higher critical buckling coefficient than the approximate buckling coefficients. The approximate critical buckling coefficients obtained from closed-form solutions are 16-27% lower than what the FEA predicts.

5.4 Estimate of ultimate strength using non-linear finite element method

The objective of the second part of the FEA was to estimate the ultimate strength of a flat plate under compression using a non-linear finite element method. In the first part of this work, the linear elastic critical buckling load was found. As was described earlier, the linear elastic buckling load was found by assuming that the plate is initially perfectly flat and buckles elastically. However, by using a non-linear finite element method, initial imperfections and inelastic behavior can be modeled. According to Zienkiewicz (1991), postbuckling behavior should be studied by the large deformation process and in order to model the buckling behavior, an initial imperfection must be imposed on the initially perfect plate. Bathe (1996) states that by using the buckled mode shape of the plate in the post-buckling analysis, the load carrying capacity of the model may correspond much better to the actual structure. In this work the postbuckling strength of the plate was found when a small increase in the load resulted in large displacements, i.e., the stiffness of the plate approached zero. The load at this point was then used as the ultimate load. The collapse of the plate was therefore a combination of both buckling and yielding. The effect of the initial imperfection was investigated by modeling different models with varying initial imperfection.

The results from the non-linear FEA were compared to an approximate method, the "effective-width" method. However, in actual engineering design work, the imperfection in the actual structure may be known or can be measured.

The ALGOR non-linear finite element software was used in this section. Next, a brief summary of the non-linear finite element method will be described.

5.4.1 Non-linear finite element method

According to Bathe (1996), a non-linear analysis should be preceded by a linear analysis to determine what nonlinearities are significant in the model. By doing this, appropriate material models and non-linear formulations can be chosen.

In linear finite element analysis it is assumed that the displacements are infinitesimally small and the material is linearly elastic (Bathe, 1996). Then, the equation to be solved in static analysis was given by Eq. 43

$$\{F\} = [K]\{d\}$$

i.e., a set of simultaneous linear equations. In solving non-linear problems, a series of successive linear approximations with corrections are required. Structural non-linear effects are classified as material and/or geometric. Material non-linearity exist when stress is not proportional to strain. If a structure experiences large deformations, its changing geometric configuration may cause the structure to respond non-linearly. In general non-linear finite element analysis, the problem is to find the equilibrium of the body corresponding to the applied loads.

The Newton-Raphson method is the basic form for most of the iterative methods used in non-linear FEA (Bathe, 1996). In this solution scheme, the effective stiffness matrix and the right hand side effective load vector of the system are updated for each equilibrium iteration within all the time / load steps. This method is very effective for problems with strong nonlinearity in that it converges quadratically with respect to the number of iterations. However, the Full Newton-Raphson method is more expensive in terms of solution time. In this work the Full Newton-Raphson method with line search was used as the iterative solution scheme. The basic idea behind a line search scheme is the following: During each equilibrium iteration, the Newton-Raphson method generates a search direction for new possible solutions, while the line search scheme is used to find a solution in that direction that minimizes the out-of-balance force error. Line searches usually help to stabilize the iterative schemes, especially near the time or load levels where rapid material property and/or geometric configuration changes occur, but line searches also add to the cost per iteration (ALGOR, Accupak manual 1994).

The time step increment is the incremental solution time step used in the non-linear finite element solution procedure. The displacement convergence tolerance is used to measure equilibrium convergence. This convergence criteria is defined by the following inequality, Bathe (1996):

$$\frac{U_n - U_{n-1}}{U_n} \leq \varepsilon_D \qquad \textbf{Eq. 47}$$

where: U_n = the global displacement vector corresponding to the n-th iteration in the current time step interval.

U_{n-1} = the global displacement vector corresponding to the (n-1)-th iteration in the current time step interval.

ε_D = displacement tolerance

An energy based method was used for the convergence criteria code for equilibrium iterations. The energy based convergence criteria combines a displacement convergence criteria and an out-of-balance load vector convergence criteria code. This convergence criteria indicates when both the displacements and forces are near the equilibrium values. The amount of work done by the out-of-balance loads on the displacement increments is compared to the initial energy increment. Convergence is reached when the following inequality is satisfied:

$$\frac{\Delta U_n \cdot \Delta F_{n-1}}{\Delta U_1 \cdot \Delta F_0} \leq \varepsilon_E \qquad \textbf{Eq. 48}$$

where: ΔU_n = the displacement increment vector corresponding to the n-th equilibrium iteration in the current time step interval

ΔU_1 = the displacement increment vector corresponding to the 1st equilibrium iteration in the current time step interval

ΔF_{n-1} = the unbalanced nodal force vector corresponding to the (n-1)-th equilibrium iteration results in the current time step interval

ΔF_0 = the initial unbalanced nodal force vector of the current time step interval

The *Total Lagrangian Formulation* is effective for elasto-plastic analysis involving large displacements, large rotation or small strain, according to Bathe (1996). In the total Lagrangian formulation all static and kinematic variables are referred to at time, t = 0. All kinematical non-linear effects are included in the total Lagrangian formulation, i.e., non-linear effects due to large displacements and large rotations.

A fundamental difference between calculating the stresses in an elastic and inelastic model is that in an elastic model the stress can be calculated from the strain alone. However, calculation of the stress in an inelastic response depends on the stress and strain history. The *von Mises material model* is based on the elasto-plastic response governed by the incremental theory of plasticity (Prandtl - Reuss equations), Mendelson (1983). Three properties are used to calculate the plastic strain:

1. Yield function, from which a yield condition is given that determines when plastic flow starts.
2. Flow rule, plastic strain increments are related to the current stresses and the stress increments.
3. Hardening rule specifies how the yield function is modified during plastic flow.

In this work, the material is modeled as bilinear (see sketch below), the effective stress - effective strain relationship is a straight line.

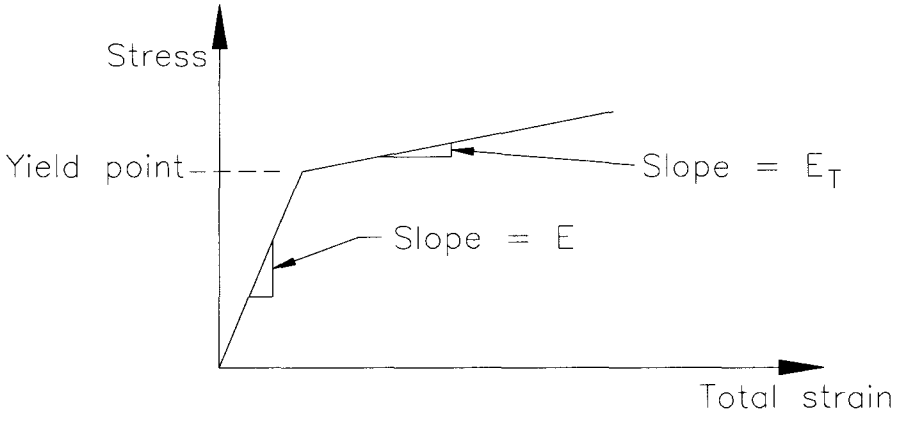

Figure 39: Bilinear material model.

where: E = modulus of elasticity

E_T = tangent modulus (strain-hardening modulus)

$\sigma_{yield\ point}$ = yield point of the material under consideration

As can be seen from the above sketch, the material model has a linear elastic behavior until the yield point of the material is reached.

5.4.2 Non-linear finite element model

In the non-linear finite element model a 3D-shell element was used; a 4-node isoparametric quadrilateral shell element. Each shell element node has five degrees of freedom, three translations and two rotations. Shown below is the plate that was analyzed using the non-linear finite element method.

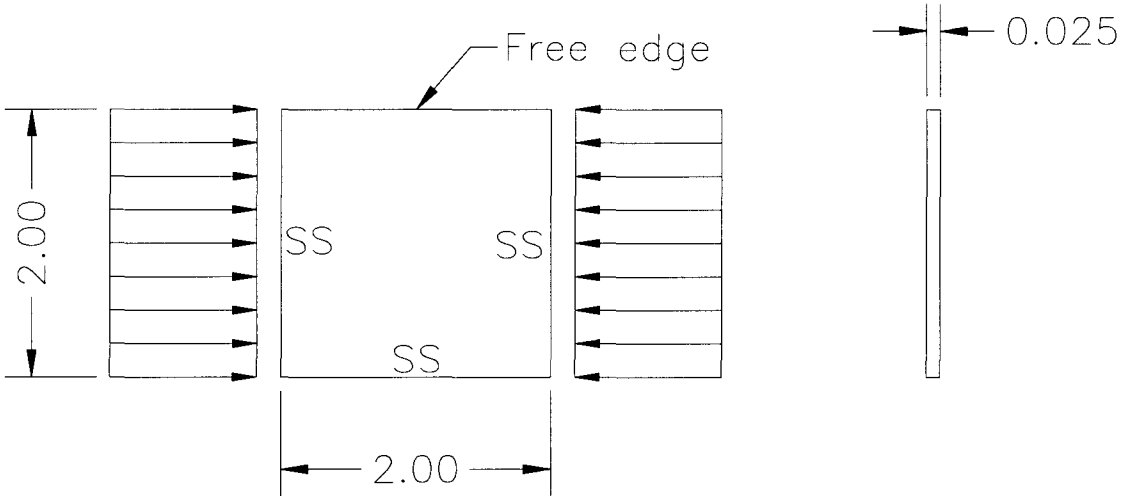

Figure 40: Sketch of non-linear finite element model.

The material properties of the above plate are shown below:

E = 30E6 psi	$E_T = 0$
$\nu = 0.3$	$\sigma_y = 36{,}000$ psi

where: E = Young's modulus

ν = Poisson's ratio

E_T = tangent modulus (strain hardening modulus)

σ_y = yield point

A sketch of the FEA-model showing boundary conditions and applied loads are shown below:

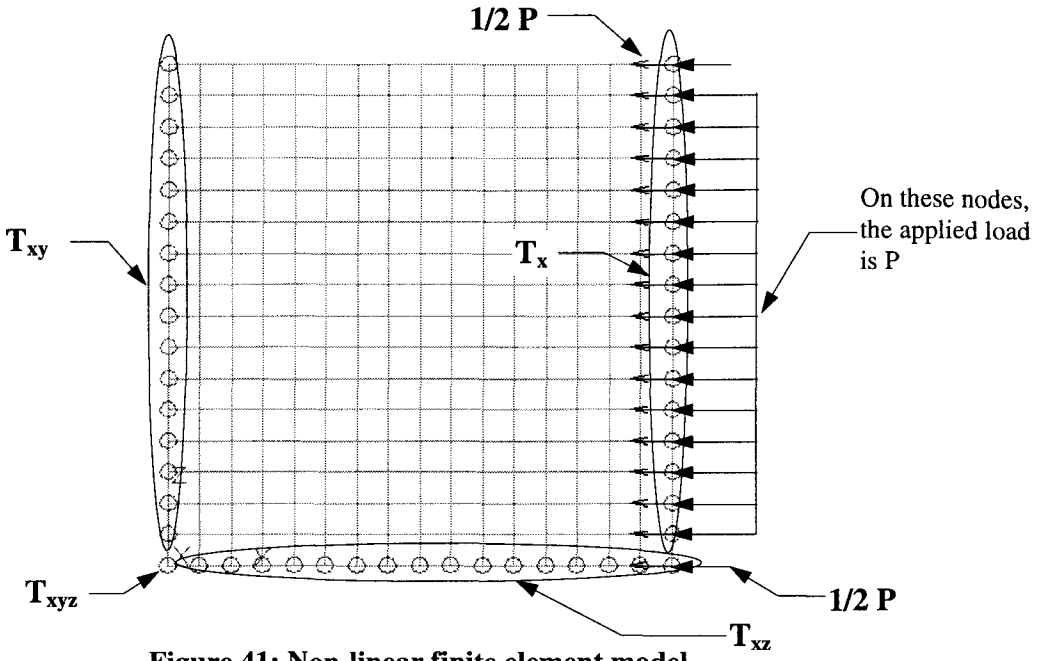

Figure 41: Non-linear finite element model.

The buckled mode shape of the flat plate being analyzed is shown below:

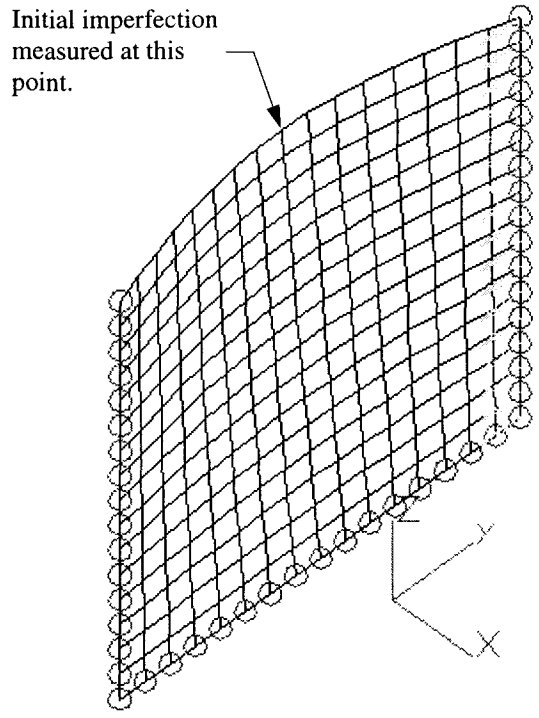

Figure 42: Buckled mode shape / initial imperfection.

The buckled mode shapes, as shown in the above picture, was then scaled down. Five different scaled-down buckled mode shapes were investigated. The imperfection was measured at the point shown in the above picture. A summary of the five models is shown below.

Length, a:	2.00 in				
Width, b:	2.00 in				
a/b - ratio:	1				
Thickness, t:	0.025 in				
Initial imperfections:	0.0125	0.0250	0.0375	0.0500	0.1000
Element type:	3D-shell				
Material model:	von Mises yield condition				
Analysis type:	Total Lagrangian				
Yield strength (psi):	36,000 psi				
Young's Modulus (psi):	30E6 psi				
Tangent modulus:	0				
No. of time steps:	50	200	100	100	100
Time step increment:	0.02000	0.00250	0.00595	0.00620	0.00800
Displacement tolerance:	0.0001				
Line search tolerance:	0.5				
Iteration method:	Full Newton Method with line search				
Convergence criteria code for equilibrium iterations:	Energy only				

Next, the results from the five non-linear FEA-models will be presented with stress dithers. The five stress dithers below all show the stresses at the last load step, i.e., the last load step before collapse of the plate. The dithered stress, in the below screen dumps, is the so called von Mises equivalent stress, and is defined as follows (Budynas, 1977):

$$\sigma_{VM} = \frac{1}{\sqrt{2}}\sqrt{(\sigma_1 - \sigma_2)^2 + (\sigma_2 - \sigma_3)^2 + (\sigma_3 - \sigma_1)^2} \qquad \textbf{Eq. 49}$$

where: σ_{VM} = von Mises equivalent 1-D stress

σ_1, σ_2, σ_3 = principal stresses ($\sigma_1 > \sigma_2 > \sigma_3$)

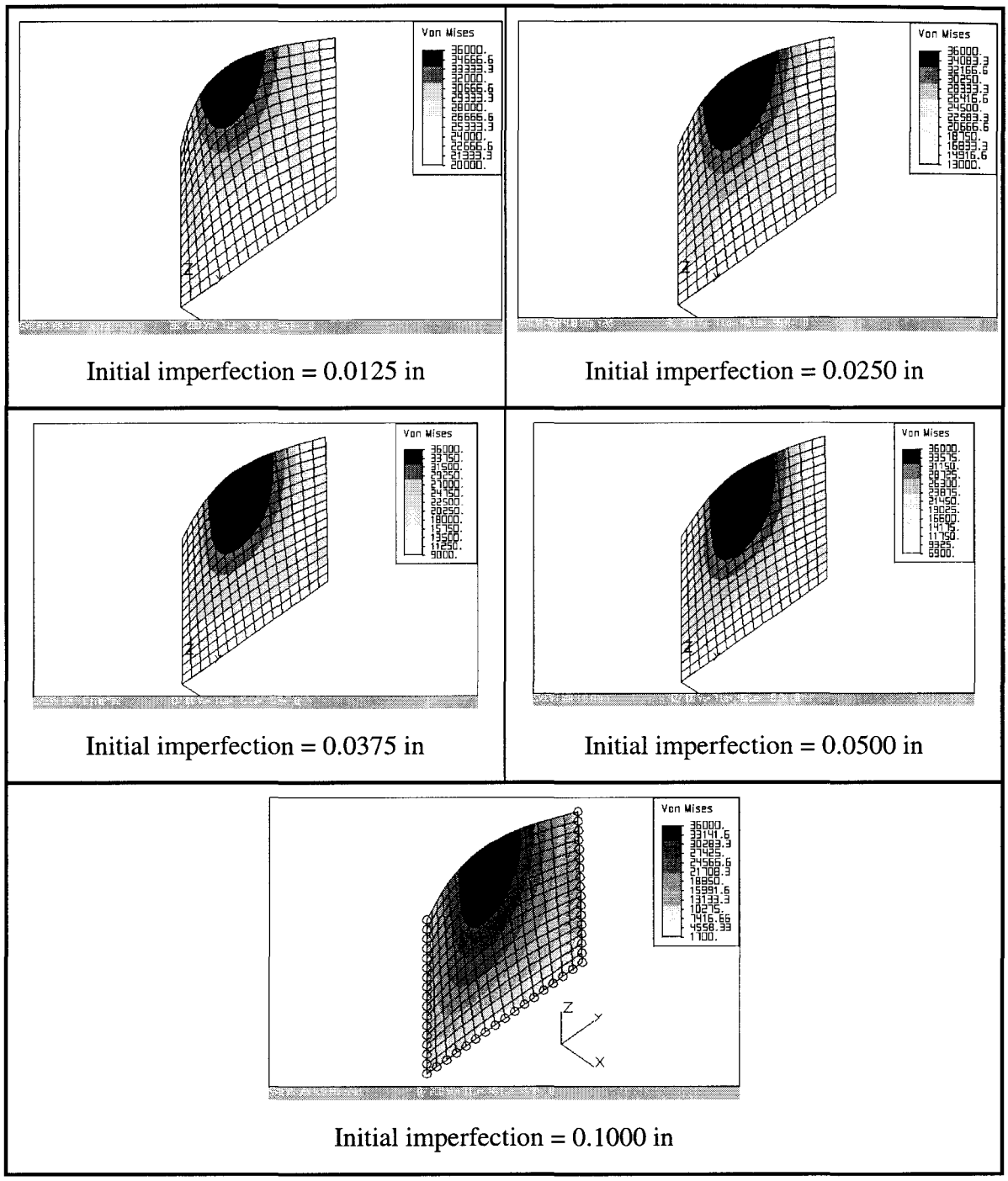

Figure 43: Stress-dithers showing the von Mises equivalent stress at the collapse load level.

Also, the stresses are the raw element stresses, i.e., the stresses have not been extrapolated to the nodes. The stresses are measured at the *Gaussian points* within each

shell element. Shown below is a shell element with four Gaussian integration points, i.e., an integration orders of 2 x 2:

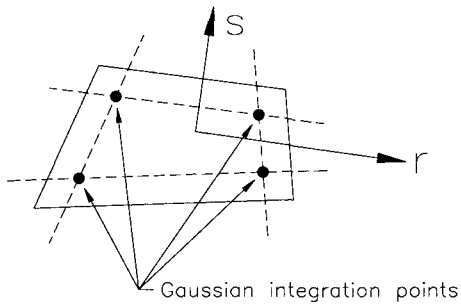

Figure 44: Sketch showing the Gaussian integration points.

The *r-s* axis is the local coordinate system of the shell element. In this work a 2 x 2 integration order was used and according to Bathe (1996), an integration order of 2 x 2 is recommended for a 4-node element.

The stress levels are indicated by the different gray scales. White color represents low stress areas and black represents high stress areas. (These kinds of stress dithers are of course in color in reality, and are easier to analyze than when they are in black and white). As can be seen from the above pictures, all the plates have large regions in the upper central part that have yielded, i.e., the black region. As was mentioned above, these stress dithers were captured at the last load step before collapse of the plate. The stiffness of the plates has dropped due to a combination of yielding and buckling. The ultimate load found by using the non-linear finite element method will next be compared to an approximate method called the "effective-width" method.

5.4.3 Estimate of the ultimate load using the "effective-width" method.

According to Galambos (1988), one method of estimating the ultimate strength of plates is by using the "effective-width" method. This method uses the fact that much of the load is carried by the regions of the plate near the edges, see sketch below:

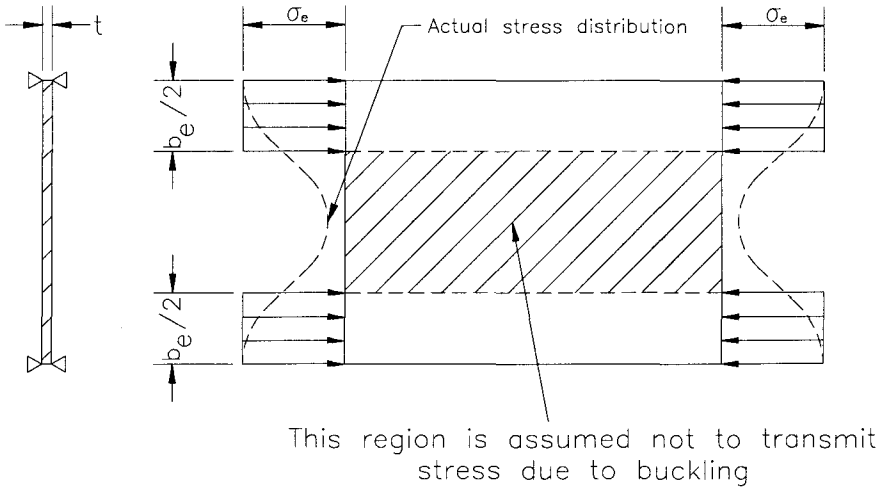

Figure 45: Sketch showing the definition of "effective-width".

The load can then be assumed to be carried by the two edge strips of the plate and the center of the plate is considered unstressed. In this work, the ultimate load of a flat plate with one free edge was to be estimated. Winter (1947) determined experimentally the "effective-width" of a flat plate under uniform compression with one free longitudinal edge as:

$$\frac{b_e}{b} = 1.19\sqrt{\frac{\sigma_c}{\sigma_e}}\left(1 - 0.30\sqrt{\frac{\sigma_c}{\sigma_e}}\right) \qquad \textbf{Eq. 50}$$

where: b_e = "effective-width"

b = width of the plate

σ_e = edge stress

σ_c = critical buckling stress

The average stress at ultimate load can then be written as:

$$\sigma_{av} = 1.19\sqrt{\sigma_c \sigma_y}\left(1 - 0.30\sqrt{\frac{\sigma_c}{\sigma_y}}\right) \qquad \textbf{Eq. 51}$$

where: $\sigma_{av} = \frac{P_{ult}}{bt}$

P_{ult} = ultimate load

b = width of the plate

t = thickness of the plate

The theoretical ultimate load for the plate that is being analyzed in this work can be calculated as follows:

$$\sigma_{av} = \frac{P_{ult}}{bt} = 1.19\sqrt{\sigma_c \sigma_y}\left(1 - 0.30\sqrt{\frac{\sigma_c}{\sigma_y}}\right) \Rightarrow P_{ult} = bt \times 1.19\sqrt{\sigma_c \sigma_y}\left(1 - 0.30\sqrt{\frac{\sigma_c}{\sigma_y}}\right)$$

$$P_{ult} = (2)(0.025)(1.19)\sqrt{6078 \times 36{,}000}\left(1 - 0.30\sqrt{\frac{6078}{36{,}000}}\right) \Rightarrow \underline{\underline{P_{ult} = 772\ lbs}}$$

5.4.4 Comparison of ultimate load obtained from FEA and from the "effective-width" method.

Shown below is a summary of the results obtained:

Initial imperfections:	0.0125	0.0250	0.0375	0.0500	0.1000
FEA:	1,152	925	771	677	422
"effective-width" estimate:	772	772	772	772	772
% diff:	49.2%	19.8%	-0.13%	-12.3%	-45.3%

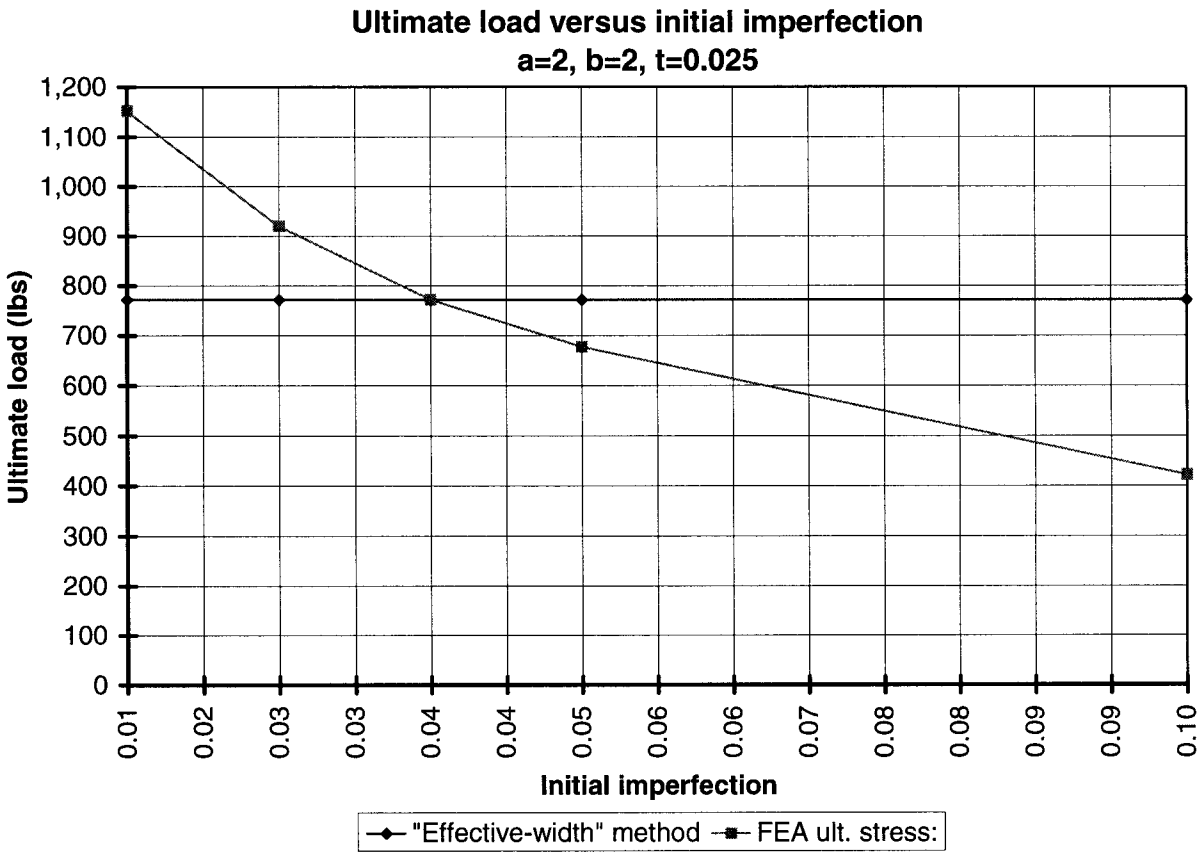

Figure 46: Ultimate strength versus initial imperfection for a flat plate with one free edge.

As can be seen in the table and graph on pages 62 and 63, the amount of initial imperfection that is imposed on the plate model strongly effects the ultimate load that the FEA predicts. The "effective-width" method does not correct for different initial imperfections, as can be seen in the above graph. With a small imperfection, the ultimate load predicted by the FEA is almost 50% higher than the "effective-width" estimate. With a large imperfection, the ultimate load predicted by the FEA is 45% lower than the "effective-width" estimate. Also, in actual engineering design work, different finite element models with varying initial imperfections should be modeled to get a feel for the behavior of the structure. In conclusion, the non-linear finite element method clearly has an advantage over the "effective-width" method in estimating the collapse load of a structure.

6. CONCLUSION

New design charts for the critical buckling coefficient for flat plates under uniform compression with non-continuous boundary conditions were presented in this work. The second part of this work was an investigation of the effect an initial geometric imperfection had on the ultimate strength of the plate, using a non-linear finite element method.

The finite element method proved to be an accurate tool to determine the critical buckling load for flat plates with complex boundary conditions. The percent error between the FEA-method and closed-form solutions were less than 6% for the plates studied in this work.

Design engineers will be able to use the design charts developed when faced with plates under compression with partial boundary conditions. By using these design charts, the engineer can find the actual critical buckling load for the entire plate (with the partial support conditions) without having to make additional approximations.

As has been shown in this work, the non-linear finite element method can be used to find the ultimate strength of plates under compression. However, the amount of initial imperfection that is imposed on the plate greatly affects the ultimate strength.

This work also showed that the non-linear finite element method was able to better predict the ultimate strength of the plate than the "effective-width" method. The "effective-width" method did not consider initial imperfections in the plate. The ultimate strength of the plate, obtained from the non-linear FEA, varied as much as 50% from the "effective-width" estimate, depending on the initial imperfection used. This indicates that it is important to accurately determine the imperfections of the structure when trying to find ultimate collapse loads. In actual engineering work, the initial imperfections may be known from manufacturing standards or from measurements of imperfections on the structure under analysis. This work also concluded that, to get an understanding of how the structure responds to different initial imperfections, several models with different imperfections should be analyzed.

7. REFERENCES

[1] Accupak Reference Manual, ALGOR, Inc., October 1994.

[2] Allen, H. G., and Bulson, P. S., *Background to Buckling*, McGraw-Hill Book Company (UK), 1980.

[3] Bergman, S., and Reissner, H., "Über die Knickung von rechteckigen Platten bei Schubbeanspruchung," *Z. Flugtech Motor-luftschiffahrt,* Vol. 23, p. 6, 1932.

[4] Bijlaard, P. P., "Buckling of Plates under Nonhomogeneous Stress," *ASCE J. Eng. Mech. Div.*, Vol. 83, No. EM3, Proc. Paper 1293, 1957.

[5] Bleich, F. and Ramsey, L. B., *A Design Manual on the Buckling Strength of Metal Structures*, Society of Naval Architects, 1951.

[6] Brockenbrough, R. L. and Johnston, B. G. *USS Steel Design Manual*, 2nd ed., U. S. Steel Corporation, Pittsburgh, Pa, 1974.

[7] Bryan, G. H. "On the Stability of a Plane Plate under Thrusts in Its Own Plane, with Applications to the 'Buckling' of the Sides of a Ship," *Proc. Lond. Math. Soc.,* Vol. 22, 1891.

[8] Budynas, R. G., *Advanced Strength and Applied Stress Analysis*, McGraw-Hill Book Company, New York, 1977.

[9] Bulson, P. S., *Stability of Flat Plates*, American Elsevier, New York, 1970.

[10] Fok, Wing-Chau, *Evaluation of Experimental Data of Plate Buckling*, ASCE, Journal of Engineering Mechanics, Vol. 110, No. 4, April 1984.

[11] Galambos, T. V. (ed.), *Guide to Stability Design Criteria for Metal Structures*, John Wiley & Sons, Inc., 1988.

[12] Gerard, G. and Becker, H., "Handbook of Structural Stability," six parts, *NACA Tech. Notes Nos. 3781-3786,* 1957 / 1958.

[13] Hamada, M. and Ota, T, *Proc. 8th Japan Nat. Congr. Appl. Mech.*, p. 103, 1958, (1959).

[14] Hamada M., Inoue, Y. and Hashimoto, H., "Buckling of Simply Supported but Partially Clamped Rectangular Plates Uniformly Compressed in One Direction," *Bulletin of the Japanese Society of Mechanical Engineers*, Vol. 10, No. 37, 1967.

[15] Heck, O. S., and Ebner, H., "Methods and Formulas for Calculating the Strength of Plate and Shell Construction as Used in Airplane Design," *Natl. Adv. Comm. Aeron., Tech. Memo. 785*, 1936.

[16] Iguchi, S., "Die Knickungen der rechteckigen Platte durch Schubkräfte," *Ing. Arch.*, Vol. 9, p. 1, 1938.

[17] Kirchhoff, *J. de Crelle*, Vol. 40, 1850.

[18] Leggett, D. M., "The Buckling of a Square Panel in Shear When One Pair of Opposite Edges Is Clamped and the Other Pair Simply Supported," *Tech. Rep. R & M No. 1991,* Aeronautical Research Council, 1941.

[19] Maulbetsch, J. L., "Buckling of Compressed Rectangular Plates with Built-in Edges," *ASME J. Appl. Mech.,* vol. 4, no. 2, June 1937.

[20] Mendelson, A., *Plasticity: Theory and Application*, Robert E. Krieger, Malabar, Florida, 1983.

[21] Moheit, W., "Schubbeulung rechteckiger Platten mit eingespannten Rändern," Thesis, Technische Hochschule Darmstadt, Leipzig, 1939.

[22] Norris, C. H., Polychrone, D. A. and Capozzoli, L. J., "Buckling of Intermittently Supported Rectangular Plates," *Welding Journal*, Vol. 30, p. 546-556, 1951.

[23] Seide, P. and Stein, M., "Compressive Buckling of Simply Supported Plates with Longitudinal Stiffeners," *NACA Tech. Note No. 1825*, 1949.

[24] Seydel, E., "Über das Ausbeulen von rechteckigen isotropen oder orthogonalan-isotropen Platten bei Scubbeanspruchung," *Ing. Arch.,* Vol. 4, p. 169, 1933.

[25] Stein, O., "Stabilität ebener Rechteckbleche unter Biegung and Schub", *Bauingenieur,* Vol. 17, p. 308, 1959.

[26] Timoshenko, S., "Einige Stabilitätsprobleme der Elastizitätstheorie," *Z. Math. Phys.,* Vol. 58, pp. 337, 1910.

[27] Timoshenko, S., " Stability of the Webs of Plate Girders," *Engineering*, Vol. 138, p. 207, 1934.

[28] Timoshenko, S., *Theory of Elastic Stability,* Engineering Societies Monograph, McGraw-Hill Book Company, 1936.

[29] Timoshenko, S. P. and Gere, J. M., *Theory of Elastic Stability,* 2nd ed., McGraw-Hill, New York, 1961.

[30] Wang, C. M., Kitipornchai, S. and Liew, K. M., "Research on Elastic Buckling of Columns, Beams and Plates: Focusing on Formulas and Design Charts," *Journal of Constructional Steel Research,* **26** (1993) 211-230.

[31] Way, S., "Stability of Rectangular Plates under Shear and Bending Forces," *J. Appl. Mech. ASME*, 1936.

[32] Winter, G. *Strength of Thin Steel Compression Flanges*, Trans. Am. Soc. Civ. Eng., Vol. 112, p. 527, 1947.

[33] Yoshizuka, J. and Narmoka, M., "Buckling Coefficient of Simply Supported Rectangular Plates under Combined Bending and Compressive Stresses in Two Perpendicular Directions," *Stahlbau*, Vol. 40, p. 217, 1971.

[34] Young, Warren, C., *Roark's Formulas for Stress & Strain*, McGraw-Hill, Inc., 1989.

[35] Zienkiewicz, O. C., *The Finite Element Method*, Vol. 2, 4th ed., McGraw-Hill Book Company (UK) Limited, 1991.